

ผลของแมงกนีเซียมออกไซด์ที่มีต่อปฏิกิริยาการเผาไหม้พาทาลิกแอนไฮไดรด์

บนตัวเร่งปฏิกิริยาออกไซด์ของโลหะทรานซิชัน



นางสาวจิตติกาญจน์ นุกูลชิต

วิทยานิพนธ์นี้เป็นส่วนหนึ่งของการศึกษาตามหลักสูตรปริญญาวิศวกรรมศาสตรมหาบัณฑิต

สาขาวิชาวิศวกรรมเคมี ภาควิชาวิศวกรรมเคมี

คณะวิศวกรรมศาสตร์ จุฬาลงกรณ์มหาวิทยาลัย

ปีการศึกษา 2545

ISBN 974-17-2003-3

ลิขสิทธิ์ของจุฬาลงกรณ์มหาวิทยาลัย

EFFECTS OF MgO ON THE COMBUSTION OF PHTHALIC ANHYDRIDE  
OVER TRANSITION METAL OXIDE CATALYSTS



Miss Jittigan Nugoolchit

สถาบันวิทยบริการ  
จุฬาลงกรณ์มหาวิทยาลัย

A Thesis Submitted in Partial Fulfillment of the Requirements  
for the Degree of Master of Engineering in Chemical Engineering  
Department of Chemical Engineering

Faculty of Engineering  
Chulalongkorn University

Academic Year 2002

ISBN 974-17-2003-3



จิตติกาญจน์ นุกูลชิต: ผลของแมกนีเซียมออกไซด์ที่มีต่อปฏิกิริยาการเผาไหม้พาทาลิกแอนไฮไดรด์บนตัวเร่งปฏิกิริยาออกไซด์ของโลหะทรานซิชัน (EFFECTS OF MgO ON THE COMBUSTION OF PHTHALIC ANHYDRIDE OVER TRANSITION METAL OXIDE CATALYSTS)

อ. ที่ปรึกษา: รศ. ดร. ธีรธร มงคลศรี, 80 หน้า. ISBN 974-17-2003-3.

ศึกษาผลของแมกนีเซียมออกไซด์ที่มีต่อสมบัติการออกซิเดชันของตัวเร่งปฏิกิริยาออกไซด์ของโลหะทรานซิชันบนตัวรองรับอลูมินา ในปฏิกิริยาการเผาไหม้สารประกอบพาทาลิกแอนไฮไดรด์ ผลการทดลองแสดงให้เห็นว่าแมกนีเซียมออกไซด์สนับสนุนการดูดซับพาทาลิกแอนไฮไดรด์ซึ่งนำไปสู่การเผาไหม้พาทาลิกแอนไฮไดรด์ที่ดีขึ้นสำหรับออกไซด์ของโลหะที่เป็นกรดและเป็นทั้งกรดและเบส (แอมโฟเทอริก) แต่สำหรับออกไซด์ที่เป็นเบสนั้น การเติมแมกนีเซียมจะทำให้การเผาไหม้ของพาทาลิกแอนไฮไดรด์ลดลง งานวิจัยยังพบว่าอัตราส่วนของออกไซด์ของโลหะทรานซิชันต่อแมกนีเซียมออกไซด์ที่เหมาะสมมีผลทำให้การดูดซับพาทาลิกแอนไฮไดรด์สอดคล้องกับความว่องไวในการเร่งปฏิกิริยาของออกไซด์ของโลหะทรานซิชัน

สถาบันวิทยบริการ  
จุฬาลงกรณ์มหาวิทยาลัย

ภาควิชา.....วิศวกรรมเคมี.....

สาขาวิชา.....วิศวกรรมเคมี.....

ปีการศึกษา.....2545.....

ลายมือชื่อนิสิต.....

ลายมือชื่ออาจารย์ที่ปรึกษา.....

# #4470246021: MAJOR CHEMICAL ENGINEERING

KEY WORD: COMBUSTION / TRANSITION METAL OXIDE CATALYSTS / PHTHALIC ANHYDRIDE / MAGNESIUM OXIDE

JITTIGAN NUGOOLCHIT : EFFECTS OF MgO ON THE COMBUSTION OF PHTHALIC ANHYDRIDE OVER TRANSITION METAL OXIDE CATALYSTS.

THESIS ADVISOR: ASSOC.PROF. THARATHON MONGKHONSI, Ph.D.  
80 pp. ISBN 974-17-2003-3.

The effects of MgO on the oxidation property of the transition metal oxide catalysts on the combustion of phthalic anhydride was investigated. The results showed that magnesium oxide promoted the adsorption of phthalic anhydride leading to better combustion of the phthalic anhydride for the acidic and amphoteric metal oxides. For the basic metal oxides, the magnesium oxide addition would decrease the combustion of phthalic anhydride. The research also found that the ratio of transition metal oxide per magnesium oxide should be at an appropriate ratio to keep a balance between the adsorption of the phthalic anhydride and the catalytic activity of the transition metal oxides.

สถาบันวิทยบริการ  
จุฬาลงกรณ์มหาวิทยาลัย

Department .....Chemical Engineering..... Student's signature .....

Field of study... Chemical Engineering ... Advisor's signature .....

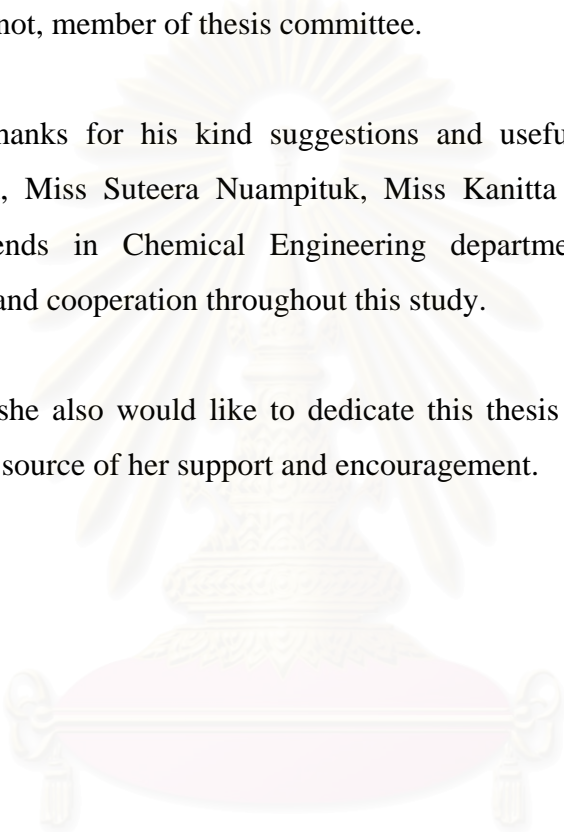
Academic year.....2002.....

## ACKNOWLEDGEMENTS

The author would like to express her greatest gratitude to her advisor, Associate Professor Tharathon Mongkhonsi, for his invaluable guidance throughout this study. Special thanks to Professor Piyasan Prasertdam for his kind supervision of this research. In addition, I would also grateful to Associate Professor Suttichai Assabumrungrat, as the chairman, Assistant Professor Supakanok Thongyai and Dr. Joongjai Panpranot, member of thesis committee.

Many thanks for his kind suggestions and useful help to Mr. Veerawat Manomaiviboon, Miss Suteera Nuampituk, Miss Kanitta Thumajariyawongsa and many best friends in Chemical Engineering department who have provided encouragement and cooperation throughout this study.

Finally, she also would like to dedicate this thesis to her parents who have always been the source of her support and encouragement.



สถาบันวิทยบริการ  
จุฬาลงกรณ์มหาวิทยาลัย

# CONTENTS

	<b>PAGE</b>
ABSTRACT (IN THAI).....	iv
ABSTRACT (IN ENGLISH).....	v
ACKNOWLEDGEMENTS.....	vi
CONTENTS.....	vii
LIST OF TABLES.....	ix
LIST OF FIGURES.....	x
CHAPTERS	
I INTRODUCTION.....	1
II LITERATURE REVIEWS.....	4
2.1 Literature reviews.....	4
2.2 Comments on previous works.....	10
III THEORY.....	11
3.1 Mechanism of oxidation reaction.....	12
3.2 Magnesium promoted transition metal oxide catalysts.....	12
3.3 Acidic and Basic Catalyst.....	13
3.4 Chemisorption at oxide surface.....	13
IV EXPERIMENTAL.....	17
4.1 Preparation of catalysts.....	18
4.2 The characterization of catalysts.....	19
4.3 The catalytic activity measurements.....	22
V RESULTS AND DISCUSSION.....	26
5.1 Catalyst characterization.....	26
5.2 Catalytic reaction.....	33
5.3 Activity and surface acidity/basicity.....	42
VI CONCLUSIONS AND RECOMMENDATIONS.....	47
6.1 Conclusions.....	47
6.2 Recommendations for future studies.....	48
REFERENCES.....	49

## CONTENTS (Cont.)

	<b>PAGE</b>
APPENDICES.....	52
Appendix A. CALCULATION OF CATALYST PREPARATION .....	53
Appendix B. CALCULATION OF DIFFUSIONAL LIMITATION EFFECT.....	56
Appendix C. CALCULATION OF SPECIFIC SURFACE AREA.....	67
Appendix D. CALIBRATION CURVE.....	70
Appendix E. DATA OF EXPERIMENT.....	72
Appendix F. MATERIAL SAFETY DATA SHEETS OF PHTHALIC ANHYDRIDE.....	75
Appendix G. PROCEDURE AND CALCULATION OF PYRIDINE AND MALEIC ANHYDRIDE ADSORPTION .....	77
VITA.....	80

สถาบันวิทยบริการ  
จุฬาลงกรณ์มหาวิทยาลัย

## LIST OF TABLES

<b>TABLES</b>	<b>PAGE</b>
3.1 Classification of solids by electrical conductivity.....	13
3.2 Classification of semiconducting metal oxides.....	14
4.1 The chemicals used in this experiment.....	18
4.2 Operating conditions for gas chromatograph (GOW-MAC).....	19
4.3 Operating conditions for gas chromatograph (GC9A) for pyridine adsorption.....	21
4.4 Operating conditions for gas chromatograph (GC9A) for maleic anhydride adsorption .....	21
4.5 Operating conditions for gas chromatographs .....	24
5.1 The composition of different magnesium loading catalysts and BET surface area.....	27
5.2 The reference XRD patterns for transition metal oxides.....	28
5.3 The relative amounts of pyridine and maleic anhydride adsorption and the amounts of absorbed pyridine and maleic anhydride of acidic metal oxides .....	43
5.4 The relative amounts of pyridine and maleic anhydride adsorption and the amounts of absorbed pyridine and maleic anhydride of amphoteric metal oxides.....	44
5.5 The relative amounts of pyridine and maleic anhydride adsorption and the amounts of absorbed pyridine and maleic anhydride of basic metal oxides.....	45

จุฬาลงกรณ์มหาวิทยาลัย

## LIST OF FIGURES

FIGURES	PAGE
4.1 Flow diagram of phthalic anhydride combustion system .....	23
5.1 The XRD pattern of chromium oxide catalysts.....	29
5.2 The XRD pattern of manganese oxide catalysts .....	29
5.3 The XRD pattern of molybdenum oxide catalysts.....	30
5.4 The XRD pattern of tungsten oxide catalysts .....	30
5.5 The XRD pattern of iron oxide catalysts.....	31
5.6 The XRD pattern of zinc oxide catalysts .....	31
5.7 The XRD pattern of copper oxide catalysts.....	32
5.8 The XRD pattern of nickel oxide catalysts.....	32
5.9 The catalytic activity of chromium oxide catalysts for the combustion of phthalic anhydride.....	34
5.10 The catalytic activity of manganese oxide catalysts for the combustion of phthalic anhydride.....	35
5.11 The catalytic activity of molybdenum oxide catalysts for the combustion of phthalic anhydride.....	36
5.12 The catalytic activity of tungsten oxide catalysts for the combustion of phthalic anhydride.....	37
5.13 The catalytic activity of iron oxide catalysts for the combustion of phthalic anhydride.....	38
5.14 The catalytic activity of zinc oxide catalysts for the combustion of phthalic anhydride.....	39
5.15 The catalytic activity of copper oxide catalysts for the combustion of phthalic anhydride.....	40
5.16 The catalytic activity of nickel oxide catalysts for the combustion of phthalic anhydride.....	41

# CHAPTER I

## INTRODUCTION

The oxidation of o-xylene to phthalic anhydride was a gas phase oxidation process. The aromatic reactant was vapourised and mixed with air in gaseous phase. The concentration of the aromatic was limited by the lower explosive limit of the gas mixture. The gas mixture then flowed to a reactor containing several thousands of catalyst tubes. The products formed, the anhydrides, were recovered by cooling the product gas stream using a condenser.

At the condenser, it was known that the lower coolant temperature, the higher product recovery. In practice, the temperature at the condenser was limited by the concentration of water in the product gas stream. If water was allowed to condense, corrosion will occur. The effluent gas leaving the condenser, therefore, still contained traces of organic compounds including the hydrocarbon reactant and the anhydride product.

Eliminating the remaining organic compounds from the effluent gas was necessary. At present, the removal could be carried out by sending the effluent gas which still contained high oxygen concentration to a furnace. This method, however, may cause problem concerning the energy balance of the plant and  $\text{NO}_x$  forming from high temperature combustion. Catalytic combustion was an alternative. There were two catalyst families that could completely oxidize organic compounds. One was the Pt-based catalysts and the other one was the acidic metal oxide based catalysts.

The Pt-based catalysts could initiate the combustion of the organic compounds at a lower temperature than the acidic metal oxide-based catalysts, typically 100-200°C lower. But the Pt-based catalysts could not withstand prolong operation in a high oxygen concentration atmosphere. The acidic metal oxide-based catalysts worked better in the latter case.

An important nature of the acidic metal oxide catalyst was its capability to adsorb acidic organic compounds. On the acidic surface, the acidic organic compounds were less likely to be adsorbed. The further oxidation of the acidic compound to combustion products, therefore, was low. Because of this reason, the acidic metal oxide catalyst became a selective oxidation catalyst for the production of anhydrides because it had low ability to further oxidise the anhydride product formed. On the contrary, this behavior caused a problem when one has to use it as a combustion catalyst.

In order to overcome the aforementioned problem, we proposed to dope a basic metal oxide compound to an acidic metal oxide catalyst to enhance the adsorption of the acidic organic compounds. However, the consideration of basic metal oxide was an important one. Too strong a basic metal oxide caused the catalyst to adsorb carbon dioxide leading to a carbonate compound formed which deactivated the catalyst. But too weak a basic metal oxide led to insufficient ability to adsorb organic acids on the catalyst.

MgO was a suitable basic metal oxide because it was not too strong a basic metal oxide until it adsorbed carbon dioxide to form a carbonate compound. But it was strong enough to adsorb organic acids [Ali *et al.* (2000)].

Transition metal oxides were technologically important materials that had found many applications. For example, in the chemical industry, these oxides were the functional components in the catalyst used in a large number of processes to convert hydrocarbons to other chemicals.

In this research the magnesium promoted transition metal oxides supported on  $\text{Al}_2\text{O}_3$  were used as catalysts for the combustion of phthalic anhydride.

In this study the Cr-Mg-O/ $\text{Al}_2\text{O}_3$ , Mn-Mg-O/ $\text{Al}_2\text{O}_3$ , Fe-Mg-O/ $\text{Al}_2\text{O}_3$ , Ni-MgO/ $\text{Al}_2\text{O}_3$ , Cu-Mg-O/ $\text{Al}_2\text{O}_3$ , Zn-Mg-O/ $\text{Al}_2\text{O}_3$ , Mo-Mg-O/ $\text{Al}_2\text{O}_3$ , and W-Mg-O/ $\text{Al}_2\text{O}_3$  catalysts with different magnesium loading had been used to investigate:

1. The oxidation properties of these catalysts for phthalic anhydride reactants.
2. The effect of different magnesium loading on the oxidation properties of these catalysts.

This present work is organized as follows:

Chapter II contains literature reviews of phthalic anhydride process, transition metal oxide and supported transition metal oxide catalysts on various reactions.

The theory of this research, studies about the oxidation reaction and its possible mechanisms, the reaction of anhydrides, and the properties of transition metal oxides are presented in chapter III.

Description of experimental systems and the operational procedures are described in chapter IV.

Chapter V reveals the experimental results of the characterization of Cr-Mg-O/Al<sub>2</sub>O<sub>3</sub>, Mn-Mg-O/Al<sub>2</sub>O<sub>3</sub>, Fe-Mg-O/Al<sub>2</sub>O<sub>3</sub>, Ni-Mg-O/Al<sub>2</sub>O<sub>3</sub>, Cu-Mg-O /Al<sub>2</sub>O<sub>3</sub>, Zn-Mg-O/Al<sub>2</sub>O<sub>3</sub>, Mo-Mg-O/Al<sub>2</sub>O<sub>3</sub>, and W-Mg-O/ Al<sub>2</sub>O<sub>3</sub> catalysts and the oxidation reaction of phthalic anhydride over these catalysts.

Chapter VI contains the overall conclusion emerged from this research.

Finally, the sample of calculation of catalyst preparation, external and internal diffusion limitations, calibration curves from area to mole of phthalic anhydride, and carbon dioxide, and data of the experiments which had emerged from this study are included in appendices at the end of this thesis.

## CHAPTER II

### LITERATURE REVIEW

The heterogeneous catalytic oxidation on transition metal oxides was extensively used in catalysis for selective and total oxidation processes. The complete catalytic oxidation was a widely used method for elimination of organic pollutants in gaseous streams to CO<sub>2</sub> and water. A large body of literature was concerned with the development of catalysis for this reaction.

This chapter reviews the works about the combustion of phthalic anhydride on Co-Mg-O/Al<sub>2</sub>O<sub>3</sub> and V-Mg-O/TiO<sub>2</sub>, the processes for recovery of phthalic anhydride, the treatment of byproducts obtained in the preparation of phthalic anhydride, the transition metal oxide and supported transition metal oxide catalysts in the various reactions.

#### 2.1 Literature reviews

Toyada and Teraji (1980) invented a process which allows the treatment of byproducts obtained in the preparation of phthalic anhydride without creating secondary pollution. Byproducts were treated by heating the byproducts to a temperature sufficient to maintain the byproducts in a molten state and thereafter atomizing air for combustion. The byproducts may be low boiling point and/or high boiling point fractions obtained in the purification step by distillation of crude phthalic anhydride produced by the partial oxidation of ortho-xylene or naphthalene.

Keuneche *et al.* (1981) invented a process for continuously separating phthalic anhydride from the reaction gases of the catalytic oxidation of o-xylene and/or naphthalene by treating reaction gas mixture with a maleic anhydride absorbent. Even though pure maleic anhydride could be used as an absorbent, maleic anhydride containing phthalic anhydride was usually used so as to keep the costs of regenerating the absorbent within economical bounds. Thus, maleic anhydride could contain up to 85% by weight phthalic anhydride. Absorption could be performed in two or more

stages, preferably in two stages. The reaction gas, with a temperature from 135 to 150°C, was introduced into the absorption zone, and withdrawn at a temperature from 45 to 80°C from the absorption zone. The maleic anhydride, which was loaded with phthalic anhydride, was separated through distillation into raw phthalic anhydride as a bottoms product and an overhead product primarily containing maleic anhydride. The overhead product was then returned to the absorption zone. The raw phthalic anhydride was treated and then purified through distillation, e.g. in a continuous, two stages distillations in which light, volatile impurities, such as residual maleic anhydride and benzoic acid, were distilled off in the first stage and the pure phthalic anhydride was distilled in the second as an overhead product. The gas leaving the absorption zone and containing small amounts of maleic anhydride was scrubbed with water. The maleic acid solution recovered from this scrubbing was evaporated, the maleic acid was dehydrated and distilled, and a part of the maleic anhydride distillate was returned into the absorption zone.

Way and Peter (1981) invented an apparatus for recovery of vaporized phthalic anhydride from the gas streams. Phthalic anhydride was recovered from gases in a multiple heat-pipe exchanger system, one or more for condensing phthalic anhydride from gases containing vapors thereof and one or more simultaneously melting out the condensed phthalic anhydride solids. The exchangers being switched in alternate cycles to melt out from the surfaces of the exchanger tube ends on which the phthalic anhydride solids were first accumulated, and to condense phthalic anhydride solids in the exchanger from which the phthalic anhydride was cleared by melting out. The cooling to recover phthalic anhydride was economical and efficient with ambient air, and the heating to melt out accumulated phthalic anhydride was effected with hot gases, such as combustion gases, preferably by incineration of residual phthalic anhydride tail gas from which phthalic anhydride was condensed, or other hot combustion gases, but other sources of heating the air or gases may be optionally substituted.

McCabe and Mitchell (1983) studied the oxidation of ethanol and acetaldehyde over alumina supported catalysts. Pt/Al<sub>2</sub>O<sub>3</sub> catalysts were only slightly more active than metal oxide catalysts for the same volume in the combustion of ethanol.

Yao (1984) studied the catalytic oxidation of ethanol at low concentrations. The catalysts used included Pt, Pd, Rh, Ag, and the first row transition metal oxide, all supported on Al<sub>2</sub>O<sub>3</sub> or ZrO<sub>2</sub>. Of the base metal oxide catalysts, CuO/ Al<sub>2</sub>O<sub>3</sub> had the highest activity for total oxidation to CO<sub>2</sub>.

Spivey (1987) reviewed the complete catalytic oxidation of volatile organics. Both metal oxides and supported noble metals are active for many deep oxidations. Metal oxide catalysts were generally less active than were supported noble metals, but they were somewhat more resistant to poisoning. This poison resistance may be due to the high active surface area of metal oxides compared to supported noble metals. The most active single metal oxide catalysts for complete oxidation for a variety of oxidation reactions were usually found to be oxides of V, Cr, Mn, Fe, Co, Ni and Cu.

Ozkan *et al.* (1990) investigated the methanol oxidation over nonprecious transition metal oxide catalysts. Catalytic oxidation of methanol was carried out over a series of the first row transition metal oxide catalysts (Cr, Mn, Fe, Co, Ni, Cu). All the catalysts exhibited similar activities for methanol conversion, but the supported copper catalyst was found to be considerably more selective to CO<sub>2</sub>.

Hess *et al.* (1993) studied catalysts containing metal oxides for use in the degenerative oxidation of organic compounds presented in exhaust gases from combustion plants. A metal oxide containing catalysts which contained oxides of titanium and/or zirconium, oxides of vanadium and/or niobium and oxides of molybdenum, tungsten, and chromium. It was found that the adding of alkaline earth metal sulfates produced a catalyst which was clearly superior to catalysts composed only of the metal oxides. The catalyst preferably contained the following components: titanium dioxide, especially in the form of anatase, vanadium oxide in the form of V<sub>2</sub>O<sub>5</sub> and tungsten oxide in the form of WO<sub>3</sub>.

Rajesh and Ozkan (1993) studied the complete oxidation of ethanol, acetaldehyde, and ethanol/methanol mixtures over copper oxide and copper-chromium oxide catalysts. For the ethanol oxidation, the temperature for 50% conversion ranged between 185 and 220°C for oxides of Cu, Cu-Cr, Cr catalysts, with the Cr catalyst requiring the lowest temperature. For 90% conversion of ethanol, the temperature ranged from 225 to 240°C with the pure Cu catalyst requiring the lowest temperature. For the acetaldehyde oxidation, CO<sub>2</sub> was the only product of acetaldehyde oxidation over oxides of Cu, Cu-Cr, Cr. Below 200°C, the Cu and the Cu-Cr catalysts, exhibited almost similar activity for acetaldehyde oxidation. The Cr/Al<sub>2</sub>O<sub>3</sub> catalyst was more active than the other two catalysts studied. Between 200 and 300°C, the catalysts exhibited a totally different behavior. The Cu catalyst was the most active for acetaldehyde oxidation. This was followed by the Cu-Cr mixed metal catalysts, while the Cr catalyst had the lowest activity. For the oxidation of a methanol-ethanol mixture, the Cr catalyst required the lowest temperature for 50% conversion. The temperature required for 90% conversion for all three catalysts ranged between 225 and 240°C, with no major difference existing between the Cu and the Cu-Cr catalysts. The Cr catalyst had a higher activity than Cu catalyst at lower temperatures, this trend was reversed at higher temperatures with Cu catalyst becoming more active.

Kang and Wan (1994) studied the effects of acid or base additives on the catalytic combustion activity of chromium and cobalt oxides. It was found that the base additive could enhance the catalytic activity of Cr, Co oxides for carbon monoxide oxidation, but the acid additive reduces the activity. For ethane combustion, the addition of a base additive to the catalysts could reduce the ethane conversion. The selectivity of carbon dioxide, however, was increased to 100% because the rate of carbon monoxide oxidation was enhanced. On the other hand, the addition of acid additive to the catalyst gave an increase in ethane conversion, but the selectivity to carbon dioxide was reduced.

Artizzu *et al.* (1999) studied the catalytic combustion of methane on alumina-supported copper oxide. It was found that deposition of CuO onto the support  $\text{MgAl}_2\text{O}_4$  led to an efficient catalyst for the total oxidation of methane with a selectivity of 100% to carbondioxide.

McCarty *et al.* (1999) investigated the stability of supported metal and supported metal oxide combustion catalysts. Durable catalysts must be able to resist the loss by vaporization. This property limited the use of noble metal and single-phase transition metal oxides as catalysts. The transition metal oxides had high volatility at high temperatures ( $>1000$  °C). Incorporation of transition metal oxides into complexes with materials such as alumina could lower their volatility by factors from 10 to 1000. The most stable catalytically active materials appeared to be Pd and  $\text{Fe}_2\text{O}_3$  and the use of these materials was recommended for long-term use in high temperature combustors.

Larsson and Andersson (2000) studied the oxides of copper, ceria promoted copper, manganese and copper manganese on  $\text{Al}_2\text{O}_3$  for the combustion of CO, ethyl acetate and ethanol. The  $\text{CuMn}_2\text{O}_4/\text{Al}_2\text{O}_3$  catalyst was more active than the  $\text{CuO}_x/\text{Al}_2\text{O}_3$  and  $\text{Mn}_2\text{O}_3/\text{Al}_2\text{O}_3$  catalyst for the complete oxidation of CO, ethyl acetate and ethanol.

Tongsang (2001) studied the oxidation property of the V-Mg-O/ $\text{TiO}_2$  catalysts on the combustion of phthalic anhydride and maleic anhydride. From the results, the MgO modified  $\text{V}_2\text{O}_5/\text{TiO}_2$  catalysts could better oxidize the anhydride ring than the unmodified one. Additionally, the appropriate ratio of vanadium per magnesium led to a balance between the adsorption of the anhydrides and the catalytic activity of vanadium and titania support.

Umpo (2001) investigated the oxidation property of the Co-Mg-O/ $\text{Al}_2\text{O}_3$  catalyst on the combustion of phthalic anhydride and maleic anhydride. The results showed that magnesium promoted the adsorption of anhydride leading to better combustion of the anhydrides. The research also found that the ratio of cobalt per

magnesium should be at an appropriate ratio to keep a balance between the adsorption of the anhydrides and the catalytic activity of cobalt and alumina support.

Cherian *et al.* (2002) studied the oxidative dehydrogenation of propane over  $\text{Cr}_2\text{O}_3/\text{Al}_2\text{O}_3$  and  $\text{Cr}_2\text{O}_3$  catalysts. It was found that bulk  $\text{Cr}_2\text{O}_3$  was efficient for complete combustion. However, when chromia was supported on another metal oxide (e.g.  $\text{Al}_2\text{O}_3$ ,  $\text{TiO}_2$ ,  $\text{SiO}_2$ ,  $\text{ZrO}_2$ ), the structure and reactivity properties were altered. The characterization with XRD indicated that all the  $\text{Cr}_2\text{O}_3/\text{Al}_2\text{O}_3$  samples had the major peaks at  $46.1$  and  $67.8^\circ$  with an additional broad peak between  $36$  and  $38^\circ$ . These peaks were due to the  $\gamma\text{-Al}_2\text{O}_3$  support. For the 20%  $\text{Cr}_2\text{O}_3/\text{Al}_2\text{O}_3$  sample, the additional peaks appeared at  $24.8$ ,  $32.8$ , and  $54.6^\circ$ , corresponding to peaks due to  $\text{Cr}_2\text{O}_3$  crystals. Thus, from the XRD it appeared that the monolayer coverage was exceeded for 20%  $\text{Cr}_2\text{O}_3/\text{Al}_2\text{O}_3$  sample.

Liu *et al.* (2002) studied the diesel soot oxidation with  $\text{NO}_2$  and  $\text{O}_2$  on supported metal oxide catalyst. Among the single oxide catalysts supported on  $\text{SiO}_2$ , oxides with relatively low melting points or high vapor pressures, such as  $\text{Re}_2\text{O}_7$ ,  $\text{MoO}_3$  and  $\text{V}_2\text{O}_5$  showed high activities.  $\text{MoO}_3/\text{SiO}_2$  was the most active catalysts among the  $\text{MoO}_3/\text{support}$  catalysts. Combination of  $\text{MoO}_3$  with  $\text{Fe}_2\text{O}_3$  and  $\text{Co}_3\text{O}_4$  deteriorated catalytic performance, whereas, combination of  $\text{CuO}$  with  $\text{MoO}_3$  or  $\text{V}_2\text{O}_5$  promoted oxidation of carbon at high temperatures.

Paola *et al.* (2002) investigated the catalytic photo-oxidation reactions with aliphatic and aromatic organic compounds having different acid strengths. The catalysts was  $\text{TiO}_2$  powders doped with various transition metal ions (Co, Cr, Cu, Fe, Mo, V and W). The co-doped powder showed to be more photoactive than the bare  $\text{TiO}_2$  for methanoic acid degradation.  $\text{TiO}_2/\text{W}$  was the most efficient sample for the photodegradation of benzoic acid and 4-nitrophenol,  $\text{TiO}_2$  the most active powder for ethanoic acid.

## 2.2 Comment on previous works

From the above reviewed literatures [e.g. Spivey (1987), Ozkan(1990)], it could be seen that transition metal oxides showed the high activity for the oxidation of organic compounds. Furthermore, the result of the combustion of phthalic anhydride using V-Mg-O/TiO<sub>2</sub> and Co-Mg-O/Al<sub>2</sub>O<sub>3</sub> as a catalysts showed that MgO could promote the adsorption of phthalic anhydride leading to better phthalic anhydride combustion [Tongsang(2001), Umpo(2001)]. The research also found that the ratio of metal per magnesium oxide should be at an appropriate ratio to keep a balance between the adsorption of phthalic anhydride and the catalytic activity of metal oxide catalysts.

From the previous reviewed literature, the following hypotheses were set

1. The phthalic anhydride combustion occurred on acidic sites.
2. Phthalic anhydride favored the adsorption on basic sites more than acidic sites.
3. The addition of basic oxide compound, MgO, not only promoted the adsorption of phthalic anhydride but also neutralized the acidic sites, the active sites for phthalic anhydride combustion.
4. Therefore, there should be a compromise between the acid site and basic site to reach a high conversion of the combustion of phthalic anhydride

In this research, the study of phthalic anhydride combustion was expanded to the other transition metal oxide catalysts. The system of transition metal oxide (chromium, manganese, iron, nickel, copper, zinc, molybdenum, and tungsten), alumina and magnesium oxide were studied the catalytic property in the combustion of phthalic anhydride.

## CHAPTER III

### THEORY

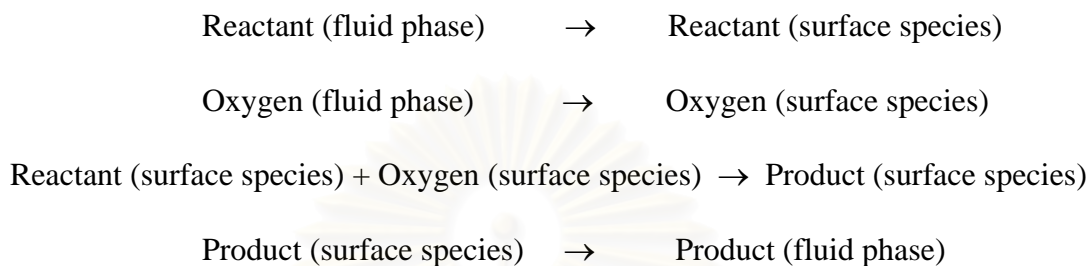
Catalytic oxidation can be categorized as complete oxidation and selective oxidation. Complete oxidation is the combustion of organic compounds to the combustion products;  $\text{CO}_2$  and  $\text{H}_2\text{O}$  [Thammanonkul (1996)]. It is a practicable method for the elimination of organic pollutants in gaseous streams. The selective oxidation is the reaction between hydrocarbon and oxygen to produce oxygenates (such as alcohols, aldehydes, carboxylic acids which are produced from partial oxidation processes) or unsaturated hydrocarbons (such as ethane and propene which can be produced from oxidative dehydrogenation process) [Thammanonkul (1996)].

In studies on oxidative catalysis, commonly great attention is attached to the state of oxygen on the catalyst surface. A relative inert oxygen molecule is activated by interacting with the surface of an oxide catalyst. The main parameter determining oxygen reactivity on the catalyst is the energy of oxygen binding with the catalyst as a thermochemical characteristic. Correlation between rates of catalytic oxidation and oxygen binding energy on oxide catalysts have been established. The weaker the oxygen binding with the catalyst surface, the more efficient is complete oxidation with this catalyst [Satterfield (1991)].

With oxide catalysts, chemisorbed surface oxygen as well as lattice oxygen may play a role. The oxidation of propylene to acrolein on a  $\text{BiMo}/\text{SiO}_2$  catalyst in a pulsed reactor showed that surface chemisorbed oxygen as well as lattice oxygen could contribute to the overall reaction. It seemed plausible that in many other cases chemisorbed oxygen would lead to a different set of products than lattice oxygen and both mechanisms could be significant. On the basis of other studies advanced the hypothesis that surface-adsorbed oxygen may in general lead to products of complete oxidation and the lattice oxygen is needed for partially oxidized products [Satterfield (1991)].

### 3.1 Mechanism of oxidation reaction

The mechanism of oxidation reaction between a reactant and an adsorbed surface oxygen species on a catalyst surface can be shown as follows:



### 3.2 Magnesium promoted transition metal oxide catalysts

Transition metal oxides were interesting materials in the field of heterogeneous catalysis. The most active single metal oxide catalysts for complete oxidation for a variety of oxidation reactions were usually found to be oxides of V, Cr, Mn, Fe, Co, Ni, and Cu. For the complete oxidation of methane, methanol, ethanol, acetaldehyde, and ethanol/methanol mixture, the transition metal oxide catalysts exhibited high activity. The  $\text{CuMn}_2\text{O}_4/\text{Al}_2\text{O}_3$  catalyst was more active than the  $\text{CuO}_x/\text{Al}_2\text{O}_3$  and  $\text{Mn}_2\text{O}_3/\text{Al}_2\text{O}_3$  catalyst for the complete oxidation of CO, ethyl acetate, and ethanol. The  $\text{MoO}_3/\text{SiO}_2$  was the most active catalysts among the  $\text{MoO}_3/\text{support}$  catalysts for the diesel soot oxidation. For the photo-oxidation of benzoic acid,  $\text{TiO}_2/\text{W}$  was the most efficient catalyst.

MgO was white powder that usually obtained by dehydration of magnesium dihydroxide. Its catalytic interest lied in its essentially basic surface character, which made it an effective catalyst support. Magnesium oxide was interesting because it had the ability to stabilize metals in unusual oxidation states and to avoid sintering and evaporation of the metal atoms [Aramendia *et al.* (1999)].

### 3.3 Acidic and Basic Catalyst [Kirk-Othmer (1979)]

The correlation of catalytic efficiency with the strength of the acid or base was of considerable importance. The general theory of acid-base catalysis in which a proton is transferred from the catalyst to the reactant (acid catalysis) or from the reactant to the catalyst (base catalysis). The velocity of the catalyzed change is thought to be determined by a protolytic reaction between the reactant and the catalyst. The molecule, on receiving or giving a proton, is converted into an unstable state which immediately (or very rapidly, compared with the velocity of the protolytic reaction) leads to the reaction under consideration. Thus, acid catalysis of a basic reactant is represented by the general scheme  $R+AH^+ \rightarrow RH^++A$ , whereas  $RH^++B \rightarrow R+BH^+$  represents basic catalysis of an acidic reactant.

### 3.4 Chemisorption at oxide surface [Bond (1987)]

On the basis of their electrical conductivities, solids are traditionally divided into four classes as shown in Table 3.1.

**Table 3.1** Classification of solids by electrical conductivity

Class	Conductivity range ( $\Omega \text{ cm}^{-1}$ )	Chemical class	Examples
Superconductors	up to $10^{35}$	metals at low temperatures	-
Conductors	$10^4$ - $10^6$	metals and alloy	Na, Ni, Cu, Pt etc.
Semiconductors	$10^3$ - $10^8$	(a) intrinsic: semi-metals (b) extrinsic: oxides and sulphides of transition and post-transition elements	Ge, Si, Ga, As etc. ZnO, Cu <sub>2</sub> O, NiO, ZnS, MoS <sub>2</sub> , NiS etc.
Insulators	$10^{-9}$ - $10^{-20}$	Stoichiometric oxides	MgO, SiO <sub>2</sub> , Al <sub>2</sub> O <sub>3</sub> etc.

Of greater interest are the oxides and sulphides whose conduction is due to their departure from precise stoichiometry: these substances are termed *extrinsic* or defect semiconductors. The more non-stoichiometric they are, the greater their conductivity. Another important general feature of semiconductors is that their conductivity increases with temperature according to a relation similar to the Arrhenius equation.

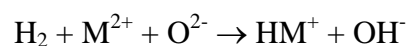
A useful generalization concerning the requirement for p-type semi-conductivity is that the cation shall have an accessible higher oxidation state: thus cobalt(II)oxide and copper(I)oxide are also in this group. For n-type semiconductivity an accessible lower oxidation state (which may include the zero-valent state) is needed: thus cadmium oxide and iron(III)oxide fall in this group (see Table 3.2).

**Table 3.2** Classification of semiconducting metal oxides

Effect of heating in air	Classification	Examples
Oxygen lost	Negative (n-type)	ZnO, Fe <sub>2</sub> O <sub>3</sub> , TiO <sub>2</sub> , CdO, V <sub>2</sub> O <sub>5</sub> , CrO <sub>3</sub> , CuO
Oxygen gained	Positive (p-type)	NiO, CoO, Cu <sub>2</sub> O, SnO, PbO, Cr <sub>2</sub> O <sub>3</sub>

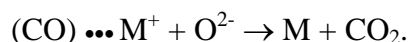
### 3.4.1 Chemisorption on semiconducting oxides

A qualitative understanding of the chemisorption of simple gases on semiconducting oxides follows simply from their chemistry. Reducing gases such as hydrogen and carbon monoxide are adsorbed strongly, but irreversibly: on heating, only water and carbondioxide respectively can be recovered. Hydrogen probably dissociates heterolytically on adsorption, viz.



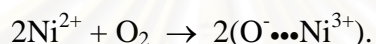
The hydroxyl ion will decompose on heating to form water and anion vacancies, and an equal number of cations will be reduced to atoms.

Carbon monoxide usually chemisorbed first on the cation, whence it reacts with an oxide ion:



Here is the first stage of a process that can lead ultimately to the complete reduction of the oxide to metal. These steps are also similar to those involved in the catalyzed oxidation of these molecules.

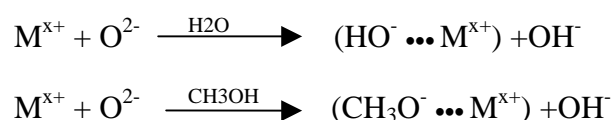
The chemisorption of oxygen on p-type oxides occurs by a mechanism involving the oxidation of  $\text{Ni}^{2+}$  ions at the surface to  $\text{Ni}^{3+}$ :



High coverages by the  $\text{O}^-$  ion can result, and it is easy to see that this is the first step in the incorporation of excess oxygen, referred to above. When the n-type oxides (exemplified by zinc oxide) are exactly stoichiometric, they cannot chemisorb oxygen: when however they are oxygen-deficient, they can chemisorb just as much as is needed to restore their stoichiometry by refilling the anion vacancies and reoxidizing the zinc atoms.

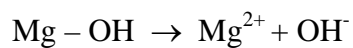
### 3.4.2 Adsorption on insulator oxides

Since the cations of insulator oxides can be neither oxidized nor reduced, they cannot chemisorb oxygen to any significant extent; they cannot chemisorb hydrogen or carbon monoxide for the same reason. They can, and do, react with water and other polar molecules as:

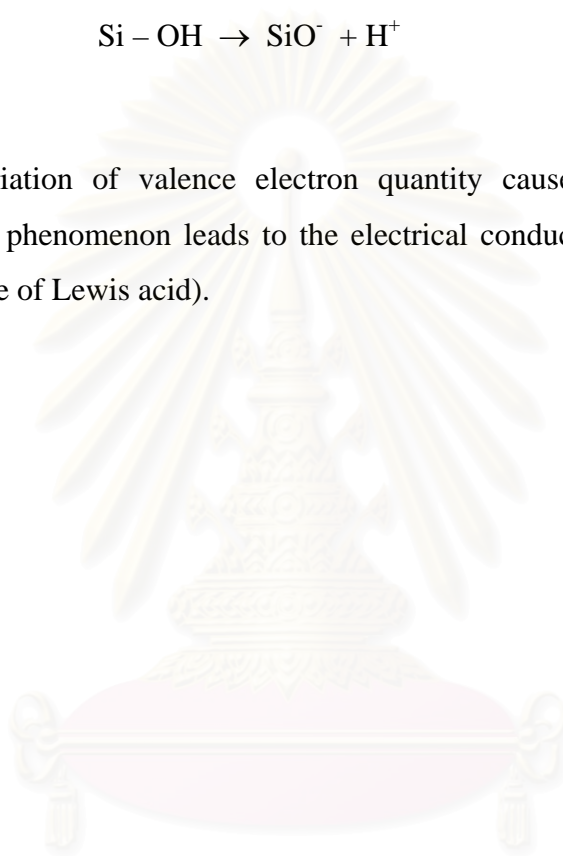


Indeed under normal circumstances the surface of oxides such as alumina and silica are covered by a layer of chemisorbed water: the surface is then said to be fully

hydroxylated, and indeed these hydroxyl groups are very firmly bound. Their complete removal by heating is almost impossible. When the oxides are suspended in water the M-OH groups can dissociate either as acids or as bases, depending on the electronegativity of the cation, e.g.



The variation of valence electron quantity causes the oxidation number change. These phenomenon leads to the electrical conductivity and acidity change (consider in case of Lewis acid).



สถาบันวิทยบริการ  
จุฬาลงกรณ์มหาวิทยาลัย

## CHAPTER IV

### EXPERIMENTAL

The experimental systems and procedures used in this work are divided into three parts:

1. The preparation of catalysts.
2. The characterization of catalysts.
3. The catalytic activity measurements.

The details of the experiments are described as the following.

#### **The scope of this study.**

The reaction conditions are chosen as follows:

Catalysts	:	Cr-Mg-O/Al <sub>2</sub> O <sub>3</sub> , Mn-Mg-O/Al <sub>2</sub> O <sub>3</sub> , Fe-Mg-O/Al <sub>2</sub> O <sub>3</sub> , Ni-Mg-O/Al <sub>2</sub> O <sub>3</sub> , Cu-Mg-O/Al <sub>2</sub> O <sub>3</sub> , Zn-Mg-O/Al <sub>2</sub> O <sub>3</sub> , Mo-Mg-O/Al <sub>2</sub> O <sub>3</sub> , W-Mg-O/Al <sub>2</sub> O <sub>3</sub>
Reactant	:	C <sub>3</sub> H <sub>4</sub> O <sub>3</sub>
Flow rate of reactant	:	100 ml/min
Reaction temperature	:	200-500°C
Space velocity	:	60000 ml g <sup>-1</sup> h <sup>-1</sup>

สถาบันวิทยบริการ  
จุฬาลงกรณ์มหาวิทยาลัย

## 4.1 Preparation of catalysts

### 4.1.1 Chemicals

The details of chemicals used in this experiment are shown in Table 4.1.

**Table 4.1** The chemicals used in this experiment.

Chemical	Grade	Supplier
Ammonium molybdate ( $(\text{NH}_4)_6\text{Mo}_7\text{O}_{24}\cdot 4\text{H}_2\text{O}$ )	Analytical	Univar, Australia
Ammonium paratungstate ( $\text{H}_{40}\text{N}_{10}\text{O}_{41}\text{W}_{12}\cdot 7\text{H}_2\text{O}$ )	Analytical	Univar, Australia
Chromium nitrate nonahydrate ( $\text{CrN}_3\text{O}_9\cdot 9\text{H}_2\text{O}$ )	Analytical	Fluka, Switzerland
Cupric nitrate trihydrate ( $\text{CuN}_2\text{O}_6\cdot 3\text{H}_2\text{O}$ )	Analytical	Fluka, Switzerland
Ferric nitrate nonahydrate ( $\text{FeN}_3\text{O}_9\cdot 9\text{H}_2\text{O}$ )	Analytical	Fluka, Switzerland
Magnesium nitrate ( $\text{Mg}(\text{NO}_3)_2$ )	Analytical	Fluka, Switzerland
Manganese nitrate tetrahydrate ( $\text{Mn}(\text{NO}_3)_2\cdot 4\text{H}_2\text{O}$ )	Analytical	Riedel-deHaen, Germany
Nickel nitrate hexahydrate ( $\text{Ni}(\text{NO}_3)_2\cdot 6\text{H}_2\text{O}$ )	Analytical	Riedel-deHaen, Germany
Zinc nitrate hexahydrate ( $\text{ZnN}_2\text{O}_6\cdot 6\text{H}_2\text{O}$ )	Analytical	Fluka, Switzerland
Alumina ( $\text{Al}_2\text{O}_3$ ) JRC ALO2 ( $\gamma$ -phase)	Japan reference catalyst	Department of Material Science, Shimane University Catalysts and Chemicals Ind. Co., Ltd.

### 4.1.2 Preparation of catalyst

Each catalyst was prepared by co-impregnation of the desired metal (Cr, Mn, Fe, Ni, Cu, Zn, Mo and W) and magnesium. 1g of Al<sub>2</sub>O<sub>3</sub> was added to an aqueous solution containing both salt of a desired metal and Mg(NO<sub>3</sub>)<sub>2</sub> at 70°C. The suspension was evaporated at 80°C, then dried in the oven at 110°C in air over night. The resulting solid was calcined in air at 550°C for 6 hours.

## 4.2 The characterization of catalysts

### 4.2.1 Determination of composition content of catalysts

The actual composition contents of all the catalysts were determined by atomic absorption spectroscopy (AAS) at the Department of Science Service Ministry of Science Technology and Environment. The calculation of the sample preparation is shown in Appendix A.

### 4.2.2 BET Surface area measurement

#### - Apparatus

The apparatus consisted of two gas feed lines for helium and nitrogen. The flow rate of gas was adjusted by means of a fine-metering valve. The sample cell was made from pyrex glass. The operation conditions of the gas chromatograph (GOW-MAC) is shown in Table 4.2.

**Table 4.2** Operation conditions of gas chromatograph (GOW-MAC)

Model	GOW-MAC
Detector	TCD
Helium flow rate	30 ml/min
Detector temperature	80°C
Detector current	80 mA

## - Procedure

The mixture of helium and nitrogen gas flowed through the system at the nitrogen relative gauge pressure of 0.3. The sample was placed in the sample cell, which was then heated up to 150°C and held at this temperature for 2 h. The sample was cooled down to room temperature and ready to measure the surface area. There were three steps to measure the surface area.

### (1) Adsorption step

The sample cell was dipped into the liquid nitrogen. Nitrogen was adsorbed on the surface of the sample until equilibrium was reached.

### (2) Desorption step

The nitrogen-adsorbed sample was dipped into the water at room temperature. The adsorbed nitrogen was desorbed from the surface of the sample. This step was completed when the recorder line return back to the base line.

### (3) Calibration step

1 ml of nitrogen gas at atmospheric pressure was injected at the calibration port and the area was measure. The area was the calibration peak.

The BET surface area was calculated using procedures described in Appendix C.

## 4.2.3 X-ray diffraction (XRD)

The phase structures of the samples were determined by X-ray diffraction, Siemens D 5000 X-ray diffractometer using  $\text{CuK}\alpha$  radiation with Ni filter in the  $2\theta$  range of 10-80°. The sample was placed into XRD plate before placing on the measured position of XRD diffractometer.

## 4.2.4 Pyridine Adsorption

The acid site of the samples were determined by the pyridine adsorption. The apparatus consisted of the tube connected to the gas chromatograph (GC9A). The condition of the gas chromatograph is shown in Table 4.3.

**Table 4.3** Operation conditions of gas chromatograph (GC9A) for pyridine adsorption

<b>Model</b>	<b>GC9A</b>
Detector	FID
Nitrogen flow rate	30 ml/min
Column temperature	150°C
Detector temperature	180°C
Injector temperature	180°C

0.02 g of sample was placed in the tube. 0.01 µl of pyridine was injected to the gas chromatograph and the area was measure. The pyridine was injected until the sample was saturated. The acid site of the sample was calculated from the total area of the pyridine adsorbed. The pyridine adsorption was calculated using the procedures described in Appendix G.

#### 4.2.5 Maleic anhydride Adsorption

The basic site of the samples were determined by the maleic anhydride adsorption. The apparatus consisted of the tube connected to the gas chromatograph (GC9A). The condition of the gas chromatograph is shown in Table 4.4.

**Table 4.4** Operation conditions of gas chromatograph (GC9A) for maleic anhydride adsorption

<b>Model</b>	<b>GC9A</b>
Detector	FID
Nitrogen flow rate	30 ml/min
Column temperature	280°C
Detector temperature	300°C
Injector temperature	300°C

0.03 g of sample was placed in the tube. 0.03  $\mu\text{l}$  of maleic anhydride aqueous solution of known concentration (0.104 g/ml) was injected to the gas chromatograph and the area was measured. The maleic anhydride was injected until the sample was saturated. The basic site of the sample was calculated from the total area of the maleic anhydride adsorbed. The maleic anhydride adsorption was calculated using the procedures described in Appendix G.

### **4.3 The catalytic activity measurements**

#### **4.3.1 Equipment**

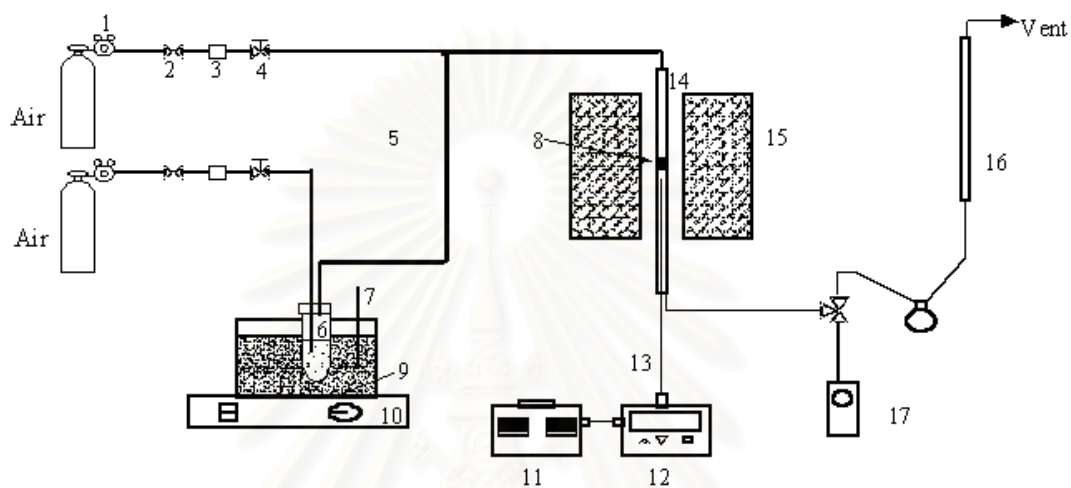
The phthalic anhydride combustion system, as shown in Figure 4.1, consists of a reactor, a saturator, an automatic temperature controller, an electrical furnace and a gas controlling system.

The reactor is made from a stainless steel tube (O.D. 3/8"). Sampling points are provided above and below the catalyst bed. Catalyst is placed between two quartz wool layers.

An automatic temperature controller consists of a magnetic contractor model Telex 87114. Reactor temperature was measured at the bottom of the catalyst bed in the reactor. The temperature control set point is adjustable within the range of 0-800°C at the maximum voltage output of 220 volt.

The electrical furnace supplies heat to the reactor for phthalic anhydride combustion. The reactor can be operated from room temperature up to 800°C at the maximum voltage of 220 volt.

The gas supplying system consists of cylinders of air zero, each equipped with pressure regulators (0-120 psig), on-off valves and fine-meter valves used for adjusting the flow rate.



- |                         |                                  |                            |
|-------------------------|----------------------------------|----------------------------|
| 1. Pressure Regulator   | 2. On-Off Valve                  | 3. Gas Filter              |
| 4. Metering Valve       | 5. Heating Line                  | 6. Saturator               |
| 7. Thermometer          | 8. Catalyst Bed                  | 9. Sand                    |
| 10. Stirring Controller | 11. Variable Voltage Transformer | 12. Temperature Controller |
| 13. Thermocouple        | 14. Reactor                      | 15. Furnace                |
| 16. Flow Meter          | 17. Sampling Point               |                            |

**Figure 4.1** Flow diagram of phthalic anhydride combustion system

The composition in the feed and product stream was analyzed by flame ionization detector gas Chromatograph Shimadzu GC9A.

A Shimadzu GC8A gas chromatograph equipped with a thermal conductivity detector was used to analyze permanent gases and water. Two columns, a 5A molecular sieve to separate oxygen and CO and a Porapak-Q column to separate CO<sub>2</sub> and water were operated in parallel. The operating conditions of the GC are listed in the Table 4.5.

**Table 4.5** Operating conditions for gas chromatographs

Gas chromatograph	GC8A	GC9A
Detector	TCD	FID
Column	MS-5A, Porapak-Q	Chromosorb WAW
Carrier gas	He (99.999%)	N <sub>2</sub> (99.999%)
Carrier gas flow	25 ml/min	30 ml/min
Column temperature	100°C	210°C
Detector temperature	130°C	250°C
Injector temperature	130°C	250°C
Analyzed gas	CO, CO <sub>2</sub> , H <sub>2</sub> O	Phthalic anhydride

#### 4.3.2 Oxidation procedure

The oxidation procedures are described in the detail below.

1. 0.1 gram of catalyst was packed in the middle of the stainless steel microreactor located in an electrical furnace.
2. The total flow rate was 100 ml/min. The concentration of phthalic anhydride in air was adjusted to the required values.
3. The reaction temperature was between 200-500°C. The effluent gas was analyzed by using the FID and TCD gas chromatograph. The chromatograph data were changed into mole of phthalic anhydride and CO<sub>2</sub> by calibration curves in Appendix D.

The operating conditions selected have been checked to confirm that there was no external and internal mass transfer resistance. The calculation was shown in Appendix B.



สถาบันวิทยบริการ  
จุฬาลงกรณ์มหาวิทยาลัย

## CHAPTER V

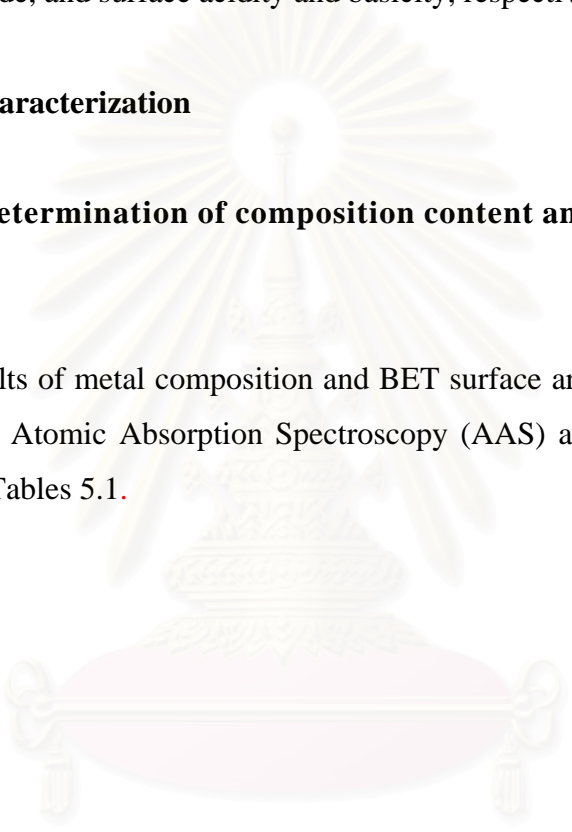
### RESULTS AND DISCUSSION

The results and discussion in this chapter are divided into two major parts including the catalyst characterization and the catalytic combustion reaction of phthalic anhydride, and surface acidity and basicity, respectively.

#### 5.1 Catalyst characterization

##### 5.1.1 Determination of composition content and BET surface area of catalyst

The results of metal composition and BET surface area of all catalysts, which are analyzed by Atomic Absorption Spectroscopy (AAS) and BET surface area are summarized in Tables 5.1.



สถาบันวิทยบริการ  
จุฬาลงกรณ์มหาวิทยาลัย

**Table 5.1** The composition of different magnesium loading catalysts and BET surface area

Catalyst	wt% metal	wt% Mg	BET surface area (m <sup>2</sup> /g)
Al <sub>2</sub> O <sub>3</sub>	-	-	130.4
8Cr-O/Al <sub>2</sub> O <sub>3</sub>	7.9	-	126.9
8Cr-1Mg-O/Al <sub>2</sub> O <sub>3</sub>	7.5	0.83	129.7
8Cr-10Mg-O/Al <sub>2</sub> O <sub>3</sub>	8.0	9.5	92.3
8Mn-O/Al <sub>2</sub> O <sub>3</sub>	8.0	-	136.3
8Mn-1Mg-O/Al <sub>2</sub> O <sub>3</sub>	8.3	1.0	104.2
8Mn-10Mg-O/Al <sub>2</sub> O <sub>3</sub>	7.8	9.8	93.3
8Mo-O/Al <sub>2</sub> O <sub>3</sub>	7.7	-	93.5
8Mo-1Mg-O/Al <sub>2</sub> O <sub>3</sub>	7.6	0.96	96.1
8Mo-10Mg-O/Al <sub>2</sub> O <sub>3</sub>	8.1	9.8	94.7
8W-O/Al <sub>2</sub> O <sub>3</sub>	7.6	-	112.7
8W-1Mg-O/Al <sub>2</sub> O <sub>3</sub>	7.7	1.0	127.0
8W-10Mg-O/Al <sub>2</sub> O <sub>3</sub>	7.9	9.7	128.6
8Fe-O/Al <sub>2</sub> O <sub>3</sub>	7.8	-	100.5
8Fe-1Mg-O/Al <sub>2</sub> O <sub>3</sub>	7.7	0.88	114.9
8Fe-10Mg-O/Al <sub>2</sub> O <sub>3</sub>	8.2	9.7	100.9
8Zn-O/Al <sub>2</sub> O <sub>3</sub>	7.9	-	132.8
8Zn-1Mg-O/Al <sub>2</sub> O <sub>3</sub>	8.1	0.87	118.4
8Zn-10Mg-O/Al <sub>2</sub> O <sub>3</sub>	7.7	9.5	97.3
8Cu-O/Al <sub>2</sub> O <sub>3</sub>	7.9	-	111.98
8Cu-1Mg-O/Al <sub>2</sub> O <sub>3</sub>	7.5	0.85	108.7
8Cu-10Mg-O/Al <sub>2</sub> O <sub>3</sub>	7.6	9.8	105.9
8Ni-O/Al <sub>2</sub> O <sub>3</sub>	7.8	-	98.4
8Ni-1Mg-O/Al <sub>2</sub> O <sub>3</sub>	7.5	0.89	107.6
8Ni-10Mg-O/Al <sub>2</sub> O <sub>3</sub>	7.8	10.0	97.0

The data in Table 5.1 indicated that the transition metal oxide and magnesium contents in the samples are close to calculated value. The correlation between the transition metal oxide and magnesium amounts and the surface area could not be defined.

### 5.1.2 X-ray Diffraction (XRD)

The first three strongest XRD peaks of transition metal oxides from the reference [The JCPDS (1980)] using CuK $\alpha$  radiation are listed in Table 5.2.

**Table 5.2** The reference XRD patterns for transition metal oxides

Oxides	Position (2 $\theta$ )	Oxides	Position (2 $\theta$ )
CrO <sub>3</sub>	14.2°, 25.8°, 26.2°	WO <sub>3</sub>	24°, 33°, 55°
Cr <sub>2</sub> O <sub>3</sub>	33.6°, 36.2°, 54.6°	WO <sub>2</sub>	25.8°, 36.8°, 37°
CrO	34.6°, 44.4°, 48°	Fe <sub>2</sub> O <sub>3</sub>	29.8°, 32.8°, 67.5°
MnO	20.2°, 21.6°, 36.4°	FeO	61°, 61.4°, 73°
MnO <sub>2</sub>	21.8°, 35.8°, 55°	ZnO	33.6°, 58.4°, 62.6°
Mn <sub>3</sub> O <sub>4</sub>	18.2°, 35.4°, 62°	ZnO <sub>2</sub>	31.8°, 37°, 63°
Mn <sub>2</sub> O <sub>3</sub>	32.2°, 35.6°, 53°	CuO	35.4°, 35.6°, 38.8°
MoO <sub>3</sub>	9.6°, 25.8°, 29.4°	Cu <sub>2</sub> O	37°, 40.4°, 42.4°
MoO <sub>2</sub>	26°, 36.8°, 53.4°	Ni <sub>2</sub> O <sub>3</sub>	32°, 44.8°, 51.6°
MgO	37°, 43°, 62.8°	NiO	37.2°, 43.2°, 62.6°

If the catalysts studied contained a transition metal oxide form, some of the peaks shown in Table 5.2 should appear in the XRD spectra. But from Figures 5.1 to 5.8, all of the catalysts investigated did not show any peak of those transition metal oxides. All of the catalysts showed the XRD patterns in the same position as Al<sub>2</sub>O<sub>3</sub> support that showed 4 peaks at 37°, 45°, 46°, and 65.5°. The peaks of these transition metal oxides were not detected possibly because the XRD patterns of these transition metal oxides were hidden by the XRD pattern of Al<sub>2</sub>O<sub>3</sub> support, the oxides did not form a crystal with significant size or it did not form a crystal.

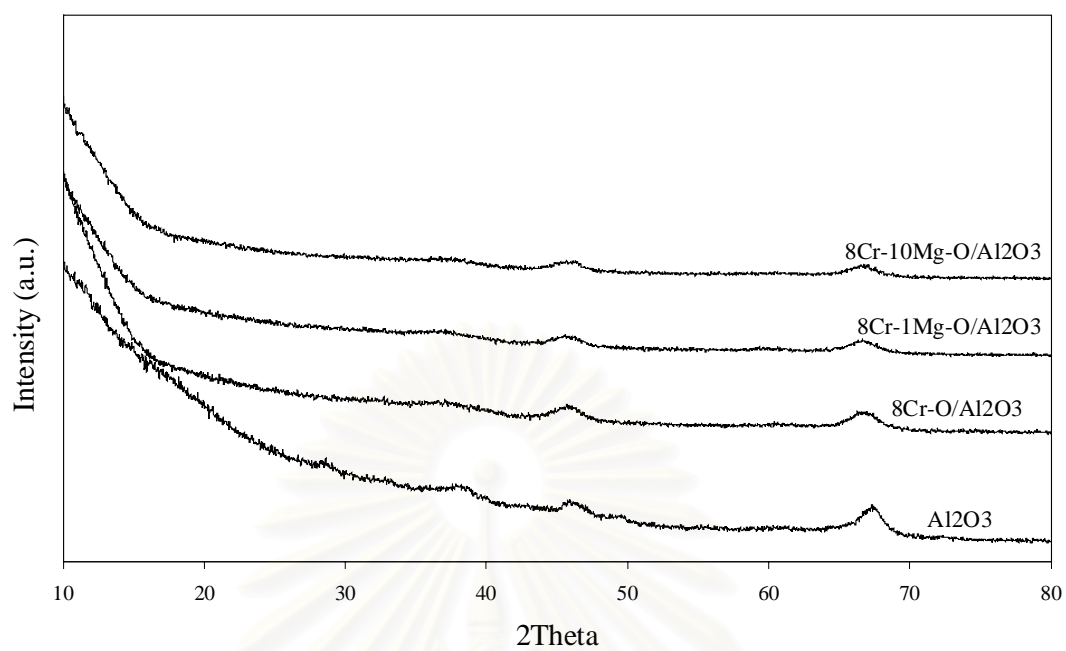


**Figure 5.1** The XRD pattern of chromium oxide catalysts

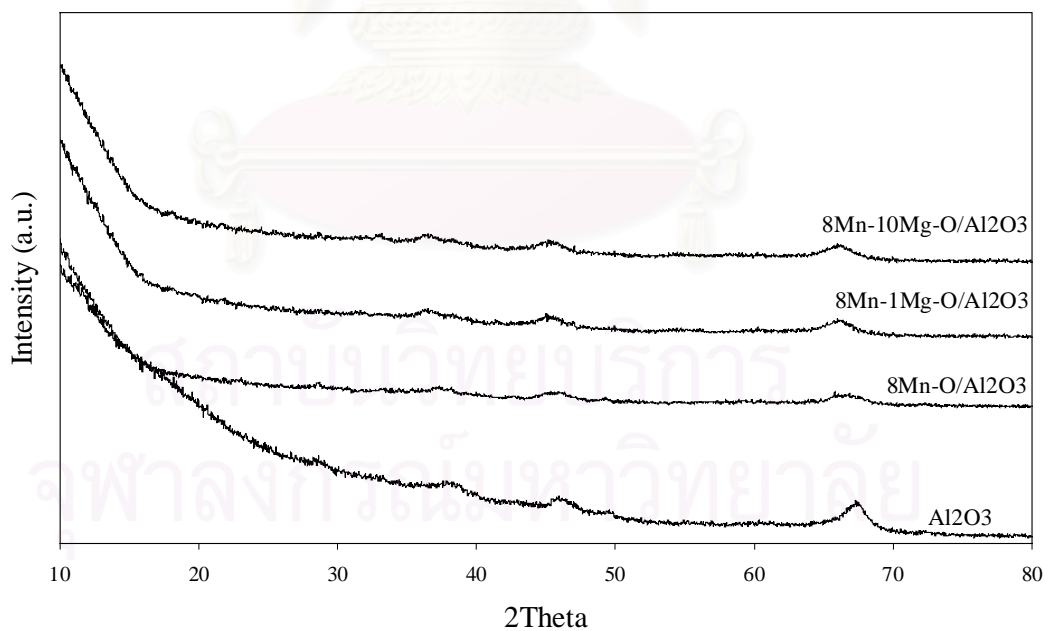


**Figure 5.2** The XRD pattern of manganese oxide catalysts

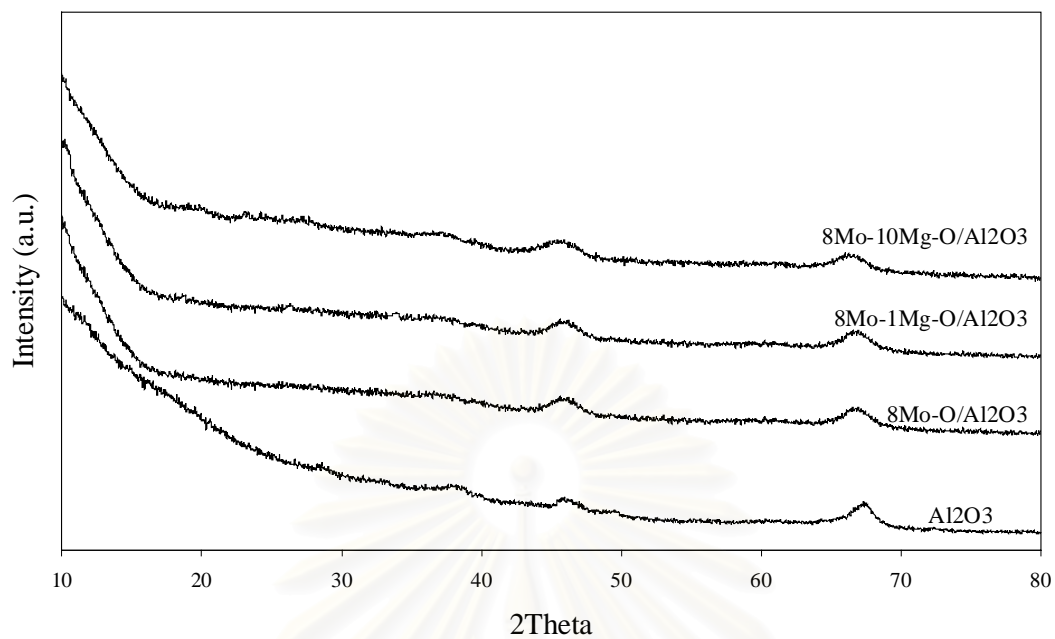


**Figure 5.3** The XRD pattern of molybdenum oxide catalysts

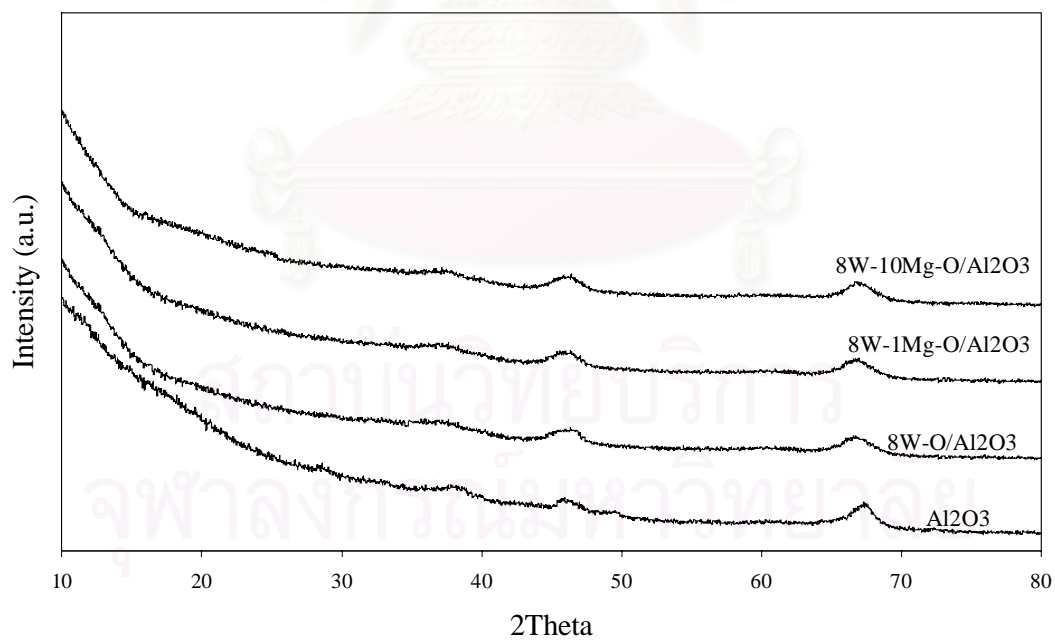


**Figure 5.4** The XRD pattern of tungsten oxide catalysts

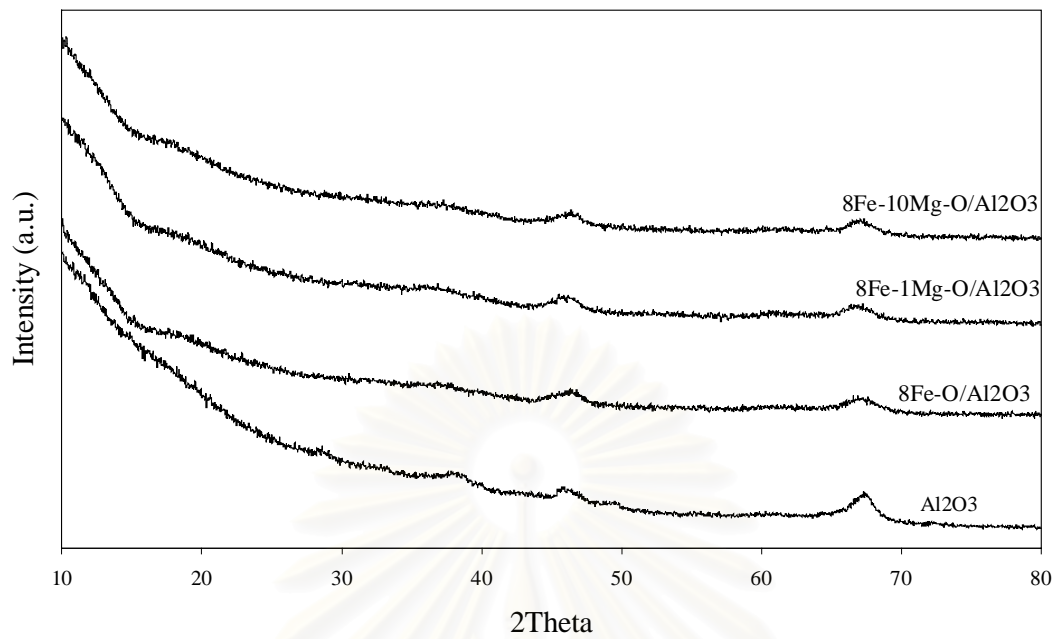


**Figure 5.5** The XRD pattern of iron oxide catalysts

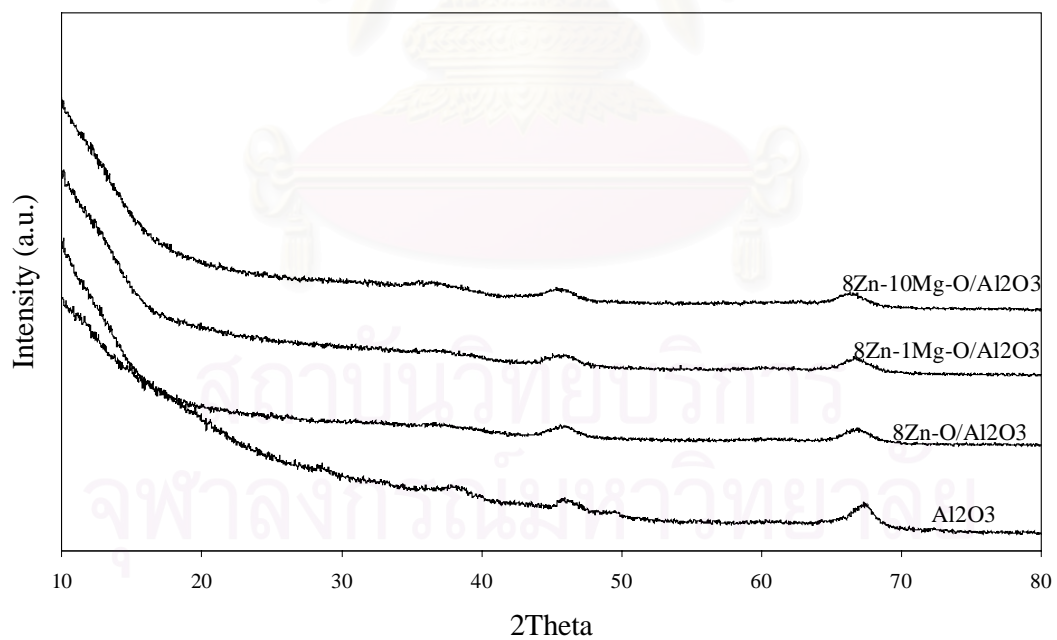


**Figure 5.6** The XRD pattern of zinc oxide catalysts

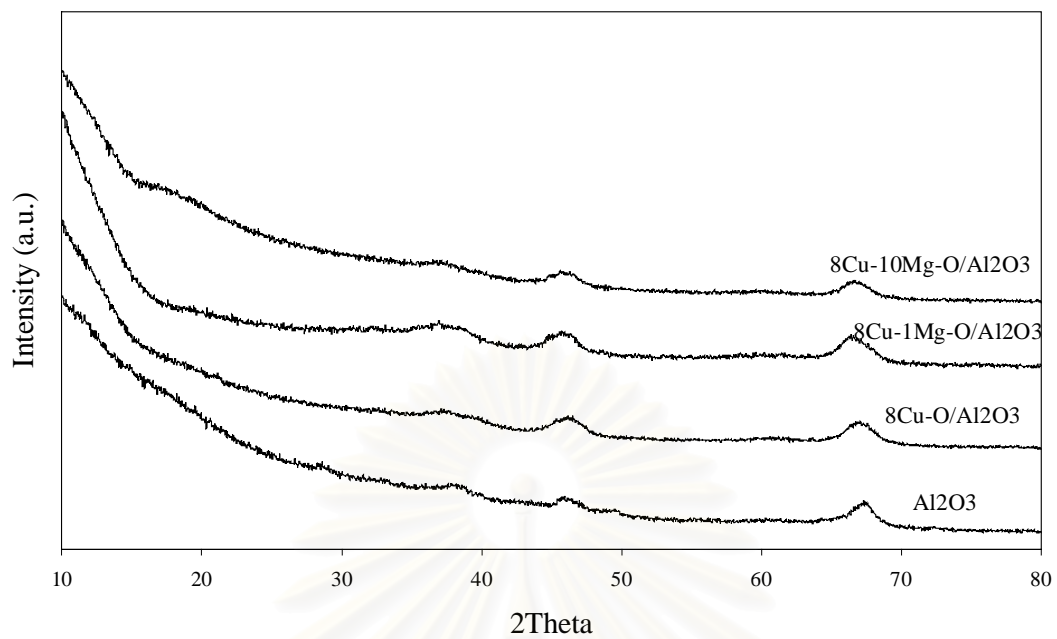


**Figure 5.7** The XRD pattern of copper oxide catalysts

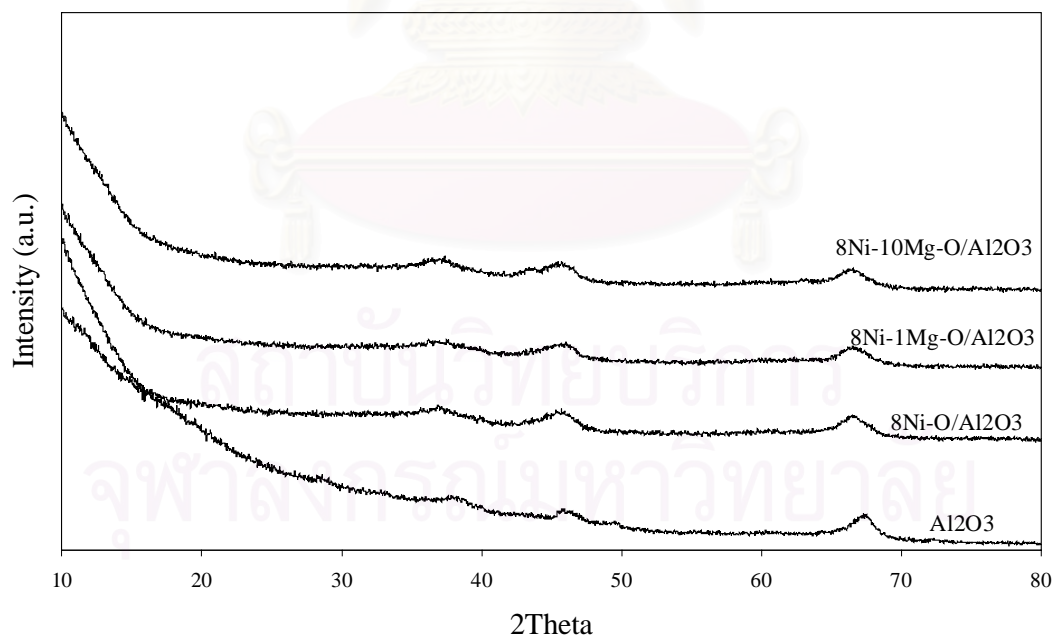


**Figure 5.8** The XRD pattern of nickel oxide catalysts

## 5.2 Catalytic reaction

Phthalic anhydride comprises of an anhydride functional group and a benzene ring. It was a product in the oxidation of o-xylene. In this work, the effects of MgO on the combustion of phthalic anhydride were received much attention. This reaction was studied in an excess oxygen atmosphere. The combustion reaction was as follows:



There were only a few studies about the combustion reaction of phthalic anhydride. The Co-Mg-O/Al<sub>2</sub>O<sub>3</sub> and V-Mg-O/TiO<sub>2</sub> were used as catalysts for this reaction. The results of using Co-Mg-O/Al<sub>2</sub>O<sub>3</sub> and V-Mg-O/TiO<sub>2</sub> catalysts showed that magnesium oxide could promote the adsorption of phthalic anhydride leading to better combustion of phthalic anhydride. Since there was no research that study the combustion of phthalic anhydride by using others transition metal oxide catalysts, the activities of other catalysts on the combustion of phthalic anhydride were studied. The chosen catalysts were the oxides of Cr, Mn, Mo, W, Fe, Zn, Cu, and Ni. These catalysts were divided into 3 groups;

Acidic transition metal oxide catalysts	:	Cr, Mn, Mo, and W
Amphoteric transition metal oxide catalysts	:	Fe, and Zn
Basic transition metal oxide catalysts	:	Cu, and Ni

From the previous research, it was observed that the ratio of the metal oxide per magnesium had some effects on the % conversion of the phthalic anhydride combustion. It was explained that an appropriate ratio would keep a balance between the adsorption of phthalic anhydride and the catalytic activity of the metal oxide catalyst.

### 5.2.1 Acidic transition metal oxide catalysts

#### - Chromium oxide catalysts

Figure 5.9 showed the phthalic anhydride conversion over chromium oxide catalysts. The amount of chromium was fixed at 8% by weight, while the amount of magnesium was varied. It was found that 8Cr-1Mg-O/Al<sub>2</sub>O<sub>3</sub> showed the best conversion, which increased from 18 to 98% in the range of temperature 200 to 400°C and raised to 100% conversion at 450°C. While 8Cr-O/Al<sub>2</sub>O<sub>3</sub> exhibited the phthalic anhydride conversion as about 2 to 94% in the temperature range 200 to 450°C and raised to 100% conversion at 500°C, 8Cr-10Mg-O/Al<sub>2</sub>O<sub>3</sub> exhibited the phthalic anhydride conversion as about 2 to 97% in the range of temperature 200 to 400°C and raised to 100% conversion at 450°C. The catalytic activity of these catalysts was in the order of 8Cr-1Mg-O/Al<sub>2</sub>O<sub>3</sub> > 8Cr-10Mg-O/Al<sub>2</sub>O<sub>3</sub> > 8Cr-O/Al<sub>2</sub>O<sub>3</sub>.

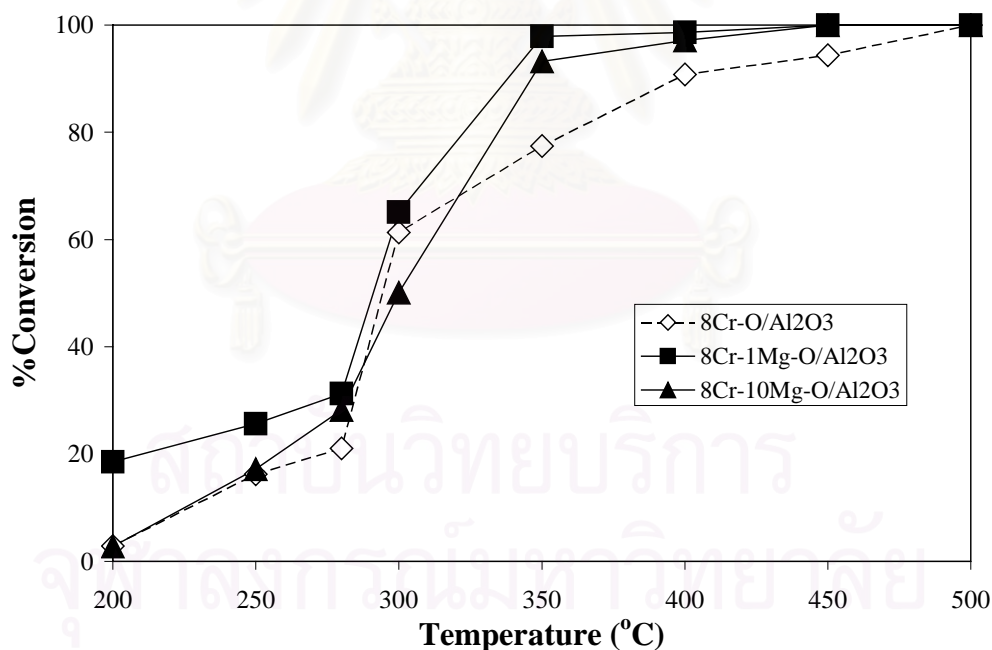


**Figure 5.9** The catalytic activity of chromium oxide catalysts for the combustion of phthalic anhydride

### - Manganese oxide catalysts

Figure 5.10 showed the phthalic anhydride conversion over manganese oxide catalysts. The amount of manganese was fixed at 8% by weight, while the amount of magnesium was varied. It was found that 8Mn-1Mg-O/Al<sub>2</sub>O<sub>3</sub> showed the best conversion, which increased from 0.8 to 95% in the range of temperature 200 to 350° C and raised to 100% conversion at 450°C. While 8Mn-O/Al<sub>2</sub>O<sub>3</sub> and 8Mn-10Mg-O/Al<sub>2</sub>O<sub>3</sub> exhibited the phthalic anhydride conversion as about 0.4 to 58% and 2 to 62%, in the range of temperature 200 to 350°C and raised to 100% conversion at 450° C and 400°C, respectively. The catalytic activity of these catalysts was in the order of 8Mn-1Mg-O/ Al<sub>2</sub>O<sub>3</sub> > 8Mn-10Mg-O/Al<sub>2</sub>O<sub>3</sub> > 8Mn-O/Al<sub>2</sub>O<sub>3</sub>.

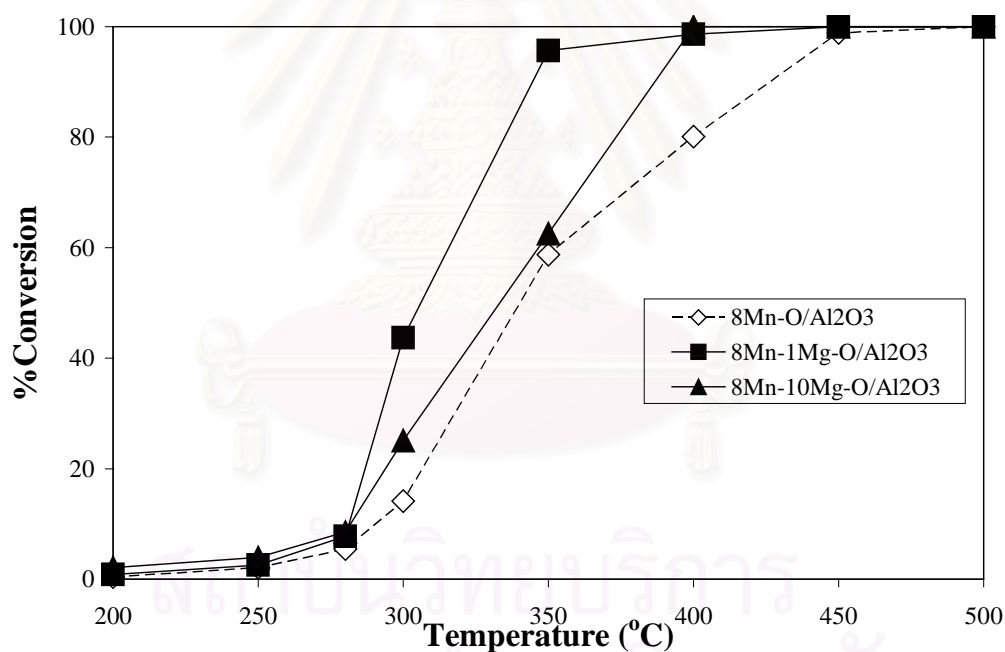


**Figure 5.10** The catalytic activity of manganese oxide catalysts for the combustion of phthalic anhydride

### - Molybdenum oxide catalysts

Figure 5.11 showed the phthalic anhydride conversion over molybdenum oxide catalysts. The amount of molybdenum was fixed at 8% by weight, while the amount of magnesium was varied. It was found that 8Mo-1Mg-O/Al<sub>2</sub>O<sub>3</sub> showed the best conversion, which increased from 0.5 to 99% in the temperature range 200 to 400°C and raised to 100% conversion at 450°C. While 8Mo-O/Al<sub>2</sub>O<sub>3</sub> and 8Mo-10Mg-O/Al<sub>2</sub>O<sub>3</sub> exhibited the phthalic anhydride conversion as about 0.4 to 72% and 1 to 86%, respectively, in the range of temperature 200 to 400°C and both raised to 100% conversion at 450°C. The catalytic activity of these catalysts was in the order of 8Mo-1Mg-O/ Al<sub>2</sub>O<sub>3</sub> > 8Mo-10Mg-O/Al<sub>2</sub>O<sub>3</sub> > 8Mo-O/Al<sub>2</sub>O<sub>3</sub>.

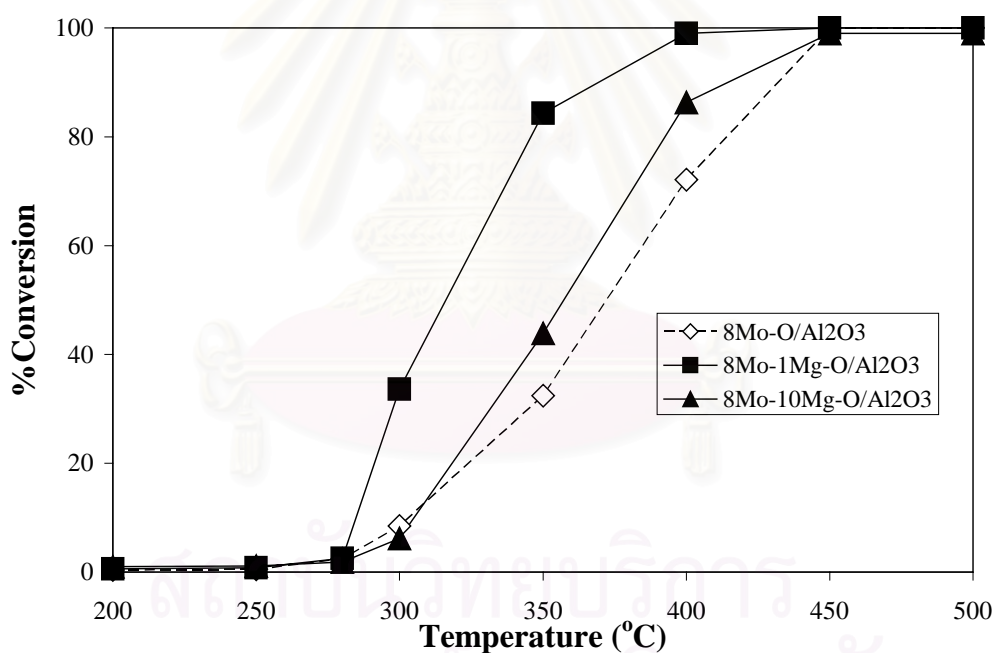


**Figure 5.11** The catalytic activity of molybdenum oxide catalysts for the combustion of phthalic anhydride

### - Tungsten oxide catalysts

Figure 5.12 showed the phthalic anhydride conversion over tungsten oxide catalysts. The amount of tungsten was fixed at 8% by weight, while the amount of magnesium was varied. It was found that 8W-1Mg-O/Al<sub>2</sub>O<sub>3</sub> showed the best conversion, which increased from 5 to 84% in the range of temperature 200 to 350°C and raised to 100% conversion at 400°C. While 8W-O/Al<sub>2</sub>O<sub>3</sub> and 8W-10Mg-O/Al<sub>2</sub>O<sub>3</sub> exhibited the phthalic anhydride conversion as about 5 to 44% and 5 to 77%, respectively, in the range of temperature 200 to 350°C and both raised to 100% conversion at 400°C. The catalytic activity of these catalysts was in the order of 8W-1Mg-O/ Al<sub>2</sub>O<sub>3</sub> > 8W-10Mg-O/Al<sub>2</sub>O<sub>3</sub> > 8W-O/Al<sub>2</sub>O<sub>3</sub>.

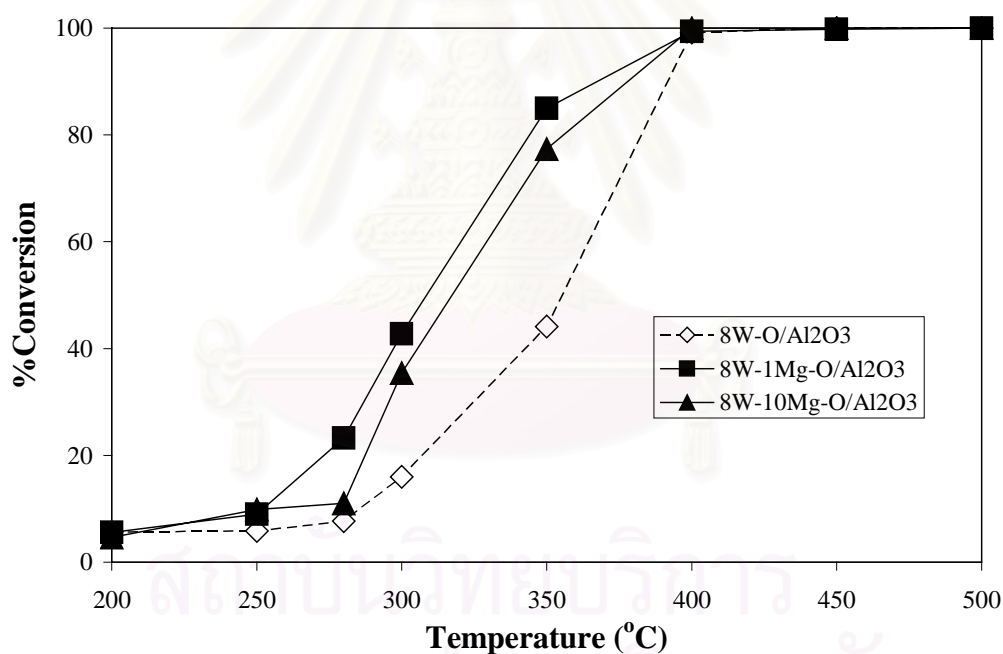


**Figure 5.12** The catalytic activity of tungsten oxide catalysts for the combustion of phthalic anhydride

## 5.2.2 Amphoteric transition metal oxide catalysts

### - Iron oxide catalysts

Figure 5.13 showed the phthalic anhydride conversion over iron oxide catalysts. The amount of iron was fixed at 8% by weight, while the amount of magnesium was varied. It was found that  $8\text{Fe-1Mg-O/Al}_2\text{O}_3$  showed the best conversion, which increased from 2 to 97% in the range of temperature 200 to 400°C and raised to 100% conversion at 450°C. While  $8\text{Fe-O/Al}_2\text{O}_3$  and  $8\text{Fe-10Mg-O/Al}_2\text{O}_3$  exhibited the phthalic anhydride conversion as about 2 to 66% and 3 to 89%, respectively, in the temperature range 200 to 400°C and both raised to 100% conversion at 450°C. The catalytic activity of these catalysts was in the order of  $8\text{Fe-1Mg-O/Al}_2\text{O}_3 > 8\text{Fe-10Mg-O/Al}_2\text{O}_3 > 8\text{Fe-O/Al}_2\text{O}_3$ .

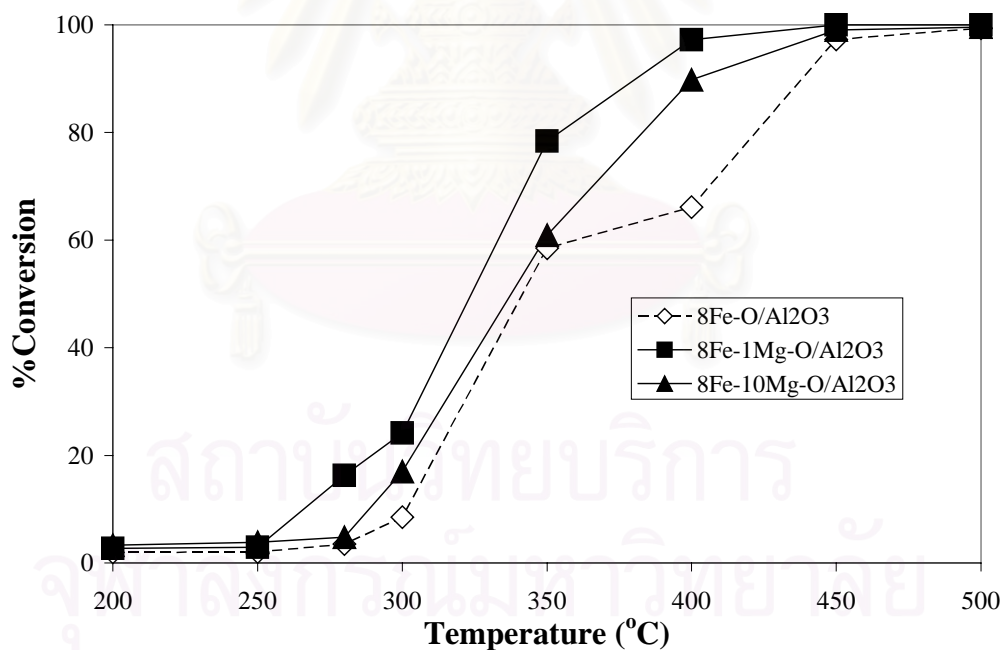


**Figure 5.13** The catalytic activity of iron oxide catalysts for the combustion of phthalic anhydride

### - Zinc oxide catalysts

Figure 5.14 showed the phthalic anhydride conversion over zinc oxide catalysts. The amount of zinc was fixed at 8% by weight, while the amount of magnesium was varied. It was found that 8Zn-1Mg-O/Al<sub>2</sub>O<sub>3</sub> showed the best conversion, which increased from 2 to 88% in the temperature range 200 to 350°C and raised to 100% conversion at 400°C. While 8Zn-O/Al<sub>2</sub>O<sub>3</sub> and 8Zn-10Mg-O/Al<sub>2</sub>O<sub>3</sub> exhibited the phthalic anhydride conversion as about 0.8 to 46% and 3 to 72% in the range of temperature 200 to 350°C and raised to 100% conversion at 450°C and 400°C, respectively. The catalytic activity of these catalysts was in the order of 8Zn-1Mg-O/Al<sub>2</sub>O<sub>3</sub> > 8Zn-10Mg-O/Al<sub>2</sub>O<sub>3</sub> > 8Zn-O/Al<sub>2</sub>O<sub>3</sub>.

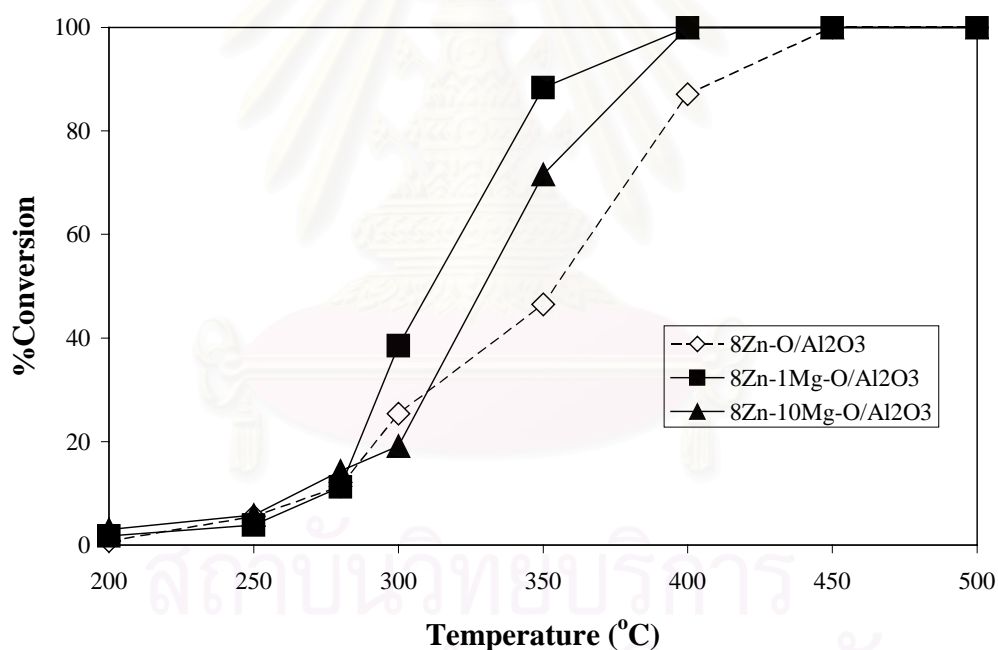


**Figure 5.14** The catalytic activity of zinc oxide catalysts for the combustion of phthalic anhydride

### 5.2.3 Basic transition metal oxide catalysts

#### - Copper oxide catalysts

Figure 5.15 showed the phthalic anhydride conversion over copper oxide catalysts. The amount of copper was fixed at 8% by weight, while the amount of magnesium was varied. It was found that  $8\text{Cu-O}/\text{Al}_2\text{O}_3$  showed the best conversion, which increased from 2 to 87% in the range of temperature 200 to 350°C and raised to 100% conversion at 450°C. While  $8\text{Cu-1Mg-O}/\text{Al}_2\text{O}_3$  and  $8\text{Cu-10Mg-O}/\text{Al}_2\text{O}_3$  exhibited the phthalic anhydride conversion as about 5 to 85% and 3 to 56%, in the range of temperature 200 to 350°C and raised to 100% conversion at 500°C and 400°C, respectively. The catalytic activity of these catalysts was in the order of  $8\text{Cu-O}/\text{Al}_2\text{O}_3 > 8\text{Cu-1Mg-O}/\text{Al}_2\text{O}_3 > 8\text{Cu-10Mg-O}/\text{Al}_2\text{O}_3$ .

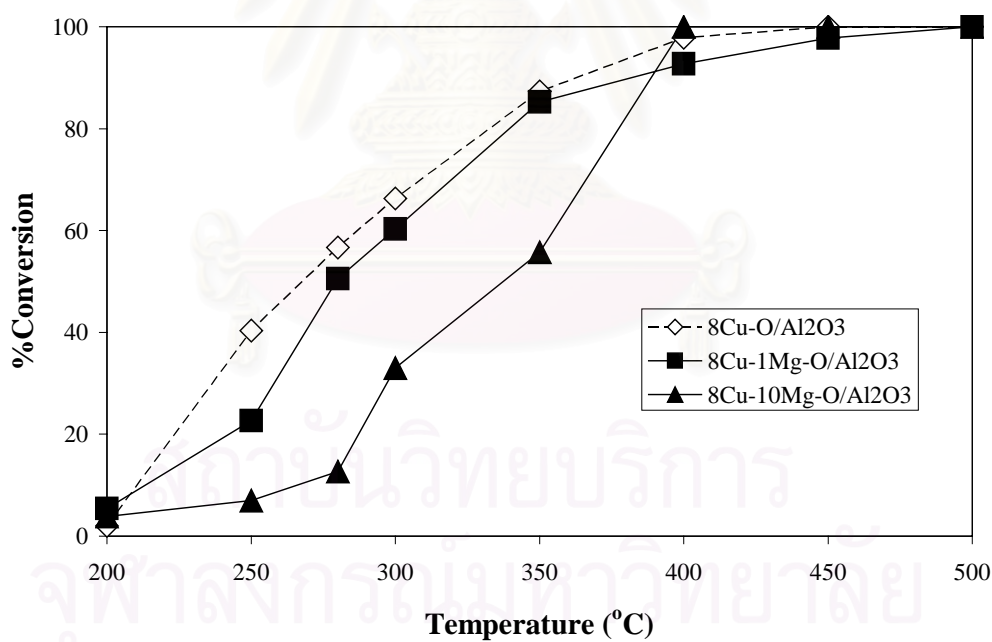


**Figure 5.15** The catalytic activity of copper oxide catalysts for the combustion of phthalic anhydride

### - Nickel oxide catalysts

Figure 5.16 showed the phthalic anhydride conversion over nickel oxide catalysts. The amount of nickel was fixed at 8% by weight, while the amount of magnesium was varied. It was found that 8Ni-O/Al<sub>2</sub>O<sub>3</sub> showed the best conversion, which increased from 3 to 96% in the range of temperature 200 to 350°C and raised to 100% conversion at 400°C. While 8Ni-1Mg-O/Al<sub>2</sub>O<sub>3</sub> and 8Ni-10Mg-O/Al<sub>2</sub>O<sub>3</sub> exhibited the phthalic anhydride conversion as about 1.4 to 95% and 1 to 85%, in the range of temperature 200 to 350°C and raised to 100% conversion at 450°C and 400°C, respectively. The catalytic activity of these catalysts was in the order of 8Ni-O/Al<sub>2</sub>O<sub>3</sub> > 8Ni-1Mg-O/Al<sub>2</sub>O<sub>3</sub> > 8Ni-10Mg-O/Al<sub>2</sub>O<sub>3</sub>.

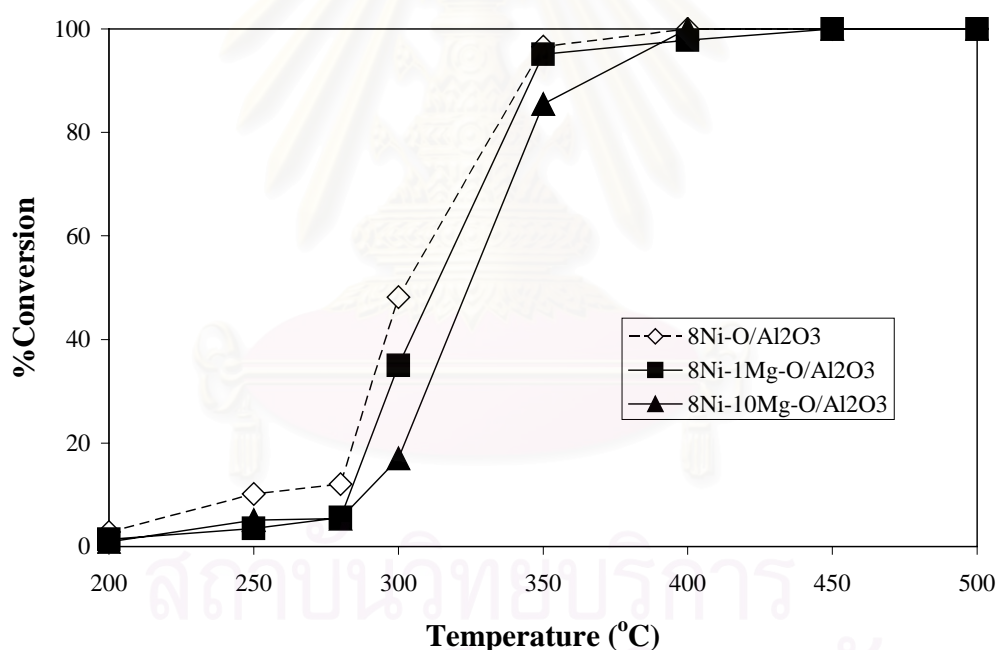


**Figure 5.16** The catalytic activity of nickel oxide catalysts for the combustion of phthalic anhydride

### 5.3 Activity and surface acidity/basicity

The surface acidity and basicity of the catalysts can be quantitatively measured by the amount of pyridine and maleic anhydride adsorption, respectively. The large amount of pyridine adsorption implies the large numbers of acid sites. The large amount of maleic anhydride adsorption implies the large numbers of basic sites. The maleic anhydride also indicated the ability of adsorption of the acidic reactant, phthalic anhydride. Thus, the large amount of maleic anhydride adsorption would have the large numbers of adsorption sites.

From the hypothesis in the previous works [Tongsang(2001), Umpo(2001)], the acid site was the active site. The basic site (MgO) would help the adsorption of the acidic reactant, but in the same time, these basic site would neutralize the acid site (active site). Thus, the maximum activity of the phthalic anhydride combustion needed the optimum between the amount of metal and MgO.

### 5.3.1 Acidic transition metal oxide catalysts

The amount of pyridine and maleic anhydride adsorption related to the  $\text{Al}_2\text{O}_3$  and the amounts of absorbed pyridine and maleic anhydride of acidic metal oxides are shown in Table 5.3.

**Table 5.3** The relative amounts of pyridine and maleic anhydride adsorption and the amounts of absorbed pyridine and maleic anhydride of acidic metal oxides

Catalyst	Pyridine adsorption		Maleic anhydride adsorption	
	Relative	(nmole/m <sup>2</sup> )	Relative	(nmole/m <sup>2</sup> )
$\text{Al}_2\text{O}_3$	1.00	0.017	1.00	6.3
8Cr-O/ $\text{Al}_2\text{O}_3$	1.30	0.022	0.92	5.8
8Cr-1Mg-O/ $\text{Al}_2\text{O}_3$	1.13	0.020	1.16	7.3
8Cr-10Mg-O/ $\text{Al}_2\text{O}_3$	0.68	0.012	1.62	10.2
8Mn-O/ $\text{Al}_2\text{O}_3$	1.96	0.034	0.67	4.2
8Mn-1Mg-O/ $\text{Al}_2\text{O}_3$	1.81	0.031	0.93	5.9
8Mn-10Mg-O/ $\text{Al}_2\text{O}_3$	0.84	0.015	1.38	8.7
8Mo-O/ $\text{Al}_2\text{O}_3$	2.13	0.037	0.63	4.0
8Mo-1Mg-O/ $\text{Al}_2\text{O}_3$	1.83	0.031	0.72	4.5
8Mo-10Mg-O/ $\text{Al}_2\text{O}_3$	0.86	0.015	0.94	5.9
8W-O/ $\text{Al}_2\text{O}_3$	1.89	0.033	0.73	4.6
8W-1Mg-O/ $\text{Al}_2\text{O}_3$	1.80	0.031	0.96	6.1
8W-10Mg-O/ $\text{Al}_2\text{O}_3$	0.71	0.012	1.56	9.8

The results of these acidic transition metal oxide catalysts agreed with the hypothesis. The acidic metal oxide catalysts had the large numbers of the active sites but had the small numbers of the adsorption sites. The addition of magnesium oxide to these acidic metal oxide catalysts would decrease the acid sites (active sites) of these acidic metal oxide catalysts. These decrements were supported by the decrements of the pyridine adsorption. Magnesium oxide would neutralize the acidic sites of the acidic metal oxide catalysts. Moreover, the increments of the maleic

anhydride adsorption indicated that the addition of magnesium oxide would increase the numbers of the basic sites of the acidic metal oxide catalysts and increase the adsorption of phthalic anhydride.

The compromise between the numbers of the active sites and the adsorption sites is important. This compromise relates to the ratio of the transition metal oxides and the magnesium, therefore the catalysts that had the optimum ratio of transition metal oxides and magnesium would have the high conversion of phthalic anhydride combustion.

### 5.3.2 Amphoteric transition metal oxide catalysts

The amount of pyridine and maleic anhydride adsorption related to the  $\text{Al}_2\text{O}_3$  and the amounts of absorbed pyridine and maleic anhydride of amphoteric metal oxides are shown in Table 5.4.

**Table 5.4** The relative amounts of pyridine and maleic anhydride adsorption and the amounts of absorbed pyridine and maleic anhydride of amphoteric metal oxides

Catalyst	Pyridine adsorption		Maleic anhydride adsorption	
	Relative	(nmole/m <sup>2</sup> )	Relative	(nmole/m <sup>2</sup> )
$\text{Al}_2\text{O}_3$	1.00	0.017	1.00	6.3
8Fe-O/ $\text{Al}_2\text{O}_3$	0.65	0.011	1.16	7.3
8Fe-1Mg-O/ $\text{Al}_2\text{O}_3$	0.60	0.010	1.43	9.0
8Fe-10Mg-O/ $\text{Al}_2\text{O}_3$	0.49	0.008	2.02	12.7
8Zn-O/ $\text{Al}_2\text{O}_3$	0.75	0.013	0.99	6.2
8Zn-1Mg-O/ $\text{Al}_2\text{O}_3$	0.70	0.012	1.26	7.9
8Zn-10Mg-O/ $\text{Al}_2\text{O}_3$	0.54	0.009	1.83	11.5

The hypothesis can also be used with these amphoteric metal oxides. The addition of magnesium oxide in appropriate quantity into the metal oxide catalysts would have the high conversion of phthalic anhydride combustion. These behaviors were like the results from using acidic transition metal oxide catalysts. The addition

of excess magnesium oxide would decrease the conversion, because magnesium oxide would neutralize the acid sites of the catalysts and the activity of the catalysts decreased.

### 5.3.3 Basic transition metal oxide catalysts

The amount of pyridine and maleic anhydride adsorption related to the  $\text{Al}_2\text{O}_3$  and the amounts of absorbed pyridine and maleic anhydride of basic metal oxides are shown in Table 5.5.

**Table 5.5** The relative amounts of pyridine and maleic anhydride adsorption and the amounts of absorbed pyridine and maleic anhydride of basic metal oxides

Catalyst	Pyridine adsorption		Maleic anhydride adsorption	
	Relative	(nmole/m <sup>2</sup> )	Relative	(nmole/m <sup>2</sup> )
$\text{Al}_2\text{O}_3$	1.00	0.017	1.00	6.3
8Cu-O/ $\text{Al}_2\text{O}_3$	0.61	0.011	1.45	9.2
8Cu-1Mg-O/ $\text{Al}_2\text{O}_3$	0.52	0.009	1.93	12.1
8Cu-10Mg-O/ $\text{Al}_2\text{O}_3$	0.46	0.008	2.77	17.4
8Ni-O/ $\text{Al}_2\text{O}_3$	0.60	0.010	2.10	13.2
8Ni-1Mg-O/ $\text{Al}_2\text{O}_3$	0.48	0.008	2.34	14.7
8Ni-10Mg-O/ $\text{Al}_2\text{O}_3$	0.44	0.007	2.95	18.6

With the result of these basic metal oxide catalysts, the hypothesis can be applicable. However, the results of these basic metal oxide catalysts were different from the results of the acidic and amphoteric metal oxide catalysts. The phthalic anhydride conversion decreased when more magnesium oxide was added into these catalysts. Because the basic metal oxide catalysts already had the small numbers of the active sites and the large number of the basic sites, when magnesium oxide was added into the basic metal oxide catalysts, the addition would decrease the numbers of the active sites and make the ability of acidic reactant adsorption and the catalytic activity unbalance. Then the combustion of phthalic anhydride decreased.

The result of pyridine and maleic anhydride adsorption showed a compromise between the catalytic activity and the adsorption of phthalic anhydride was required to achieve the maximum catalytic activity for phthalic anhydride combustion. The loss of the active site due to MgO addition could be compensated by more reactant on the surface. This phenomenon is obvious with the oxides of chromium, manganese, molybdenum and tungsten which are acidic transition metal oxides and the oxides of iron and zinc which are amphoteric transition metal oxides. For the basic transition metal oxides investigated, copper and nickel, the addition of MgO further decreased the number of the active sites, which was already small number. Therefore, the phthalic anhydride conversion decreased.



สถาบันวิทยบริการ  
จุฬาลงกรณ์มหาวิทยาลัย

## CHAPTER VI

### CONCLUSIONS AND RECOMMENDATIONS

#### 6.1 Conclusions

The conclusions of the present research are the following:

1. For phthalic anhydride combustion, magnesium played the role as promoter for acidic and amphoteric transition metal oxide catalysts.
2. The amount of transition metal oxide and magnesium in the catalyst had the effects on the catalytic activity for phthalic anhydride combustion.
3. The addition of MgO into the acidic metal oxide catalysts (oxides of chromium, manganese, molybdenum and tungsten) in the appropriate amount would increase the % conversion of phthalic anhydride combustion.
4. The addition of MgO into the amphoteric metal oxide catalysts (oxides of iron and zinc) in the appropriate amount would increase the % conversion of phthalic anhydride combustion.
5. The addition of MgO into the basic metal oxide catalysts (oxides of copper and nickel) would decrease the % conversion of phthalic anhydride combustion.

จุฬาลงกรณ์มหาวิทยาลัย

## 6.2 Recommendations for future studies

From the previous conclusions, the following recommendations for future studies can be proposed.

1. It is interesting to study the combustion of phthalic anhydride by using the other catalysts such as the used catalysts in the production of phthalic anhydride that promoted with MgO or other transition metal oxides.

2. Transition metal oxide catalysts were suitable to use in the catalytic combustion of phthalic anhydride. Therefore, it is interesting to further study the oxidation property of these catalysts with other anhydrides.



## REFERENCES

- Ali, N., Lu, C. and Masel R., "Catalytic oxidation of odorous organic acids", *Catalysis Today*, 2000, **62**, 347-353.
- Anderson, J.R., and Pratt, K.C., *Introduction to characterization and testing of catalyst*, Sydney, Academic Press, 1985.
- Aramendia, M. A., Benitez, J. A., Borau, V., Jimenez, C., Marinas, J. M., Ruiz, J. R. and Urbano, F., "Study of MgO and Pt/MgO systems by XRD, TPR, and H MAS NMR", *Langmuir*, 1999, **15**, 1192-1197.
- Artizzu, P., Garboeski, E., Primet, M., Brulle, Y., and Just, J.S., "Catalytic combustion of methane on alumina-supported copper oxide" *Catalysis Today*, 1999, **47**, 83-93.
- Bond, G. C., *Heterogeneous Catalysis principles and applications: Chemisorption at oxide surfaces*, Oxford: Clarendon Press, 1987.
- Cherian, M.; Rao, M.S.; Yang, W.T.; Jehng, J.M.; Hirt, A.M.; and Deo, G., "Oxidative dehydrogenation of propane over Cr<sub>2</sub>O<sub>3</sub>/Al<sub>2</sub>O<sub>3</sub> and Cr<sub>2</sub>O<sub>3</sub> catalysts : effect of loading, precursor and surface area", *Appl. Catal. A*, 2002, **233**, 21-33.
- Hess, K.; Morsbach, B.; Drews, R.; Buechele, W.; and Schachner, H., "Catalyst containing metal oxides for use in the degenerative oxidation of organic compounds present in exhaust gases from combustion plants" *United States Patent*, 1993, **5227356**, 1-20.
- Kang, Y.M., and Wan, B.Z., "Effects of acid or base additives on the catalytic combustion activity of chromium and cobalt oxide" *Appl. Catal. A*, 1994, **114**, 35-49.
- Keuneche, G., Klopfer, A., and Sterck, L., "Process for continuously separating phthalic anhydride from the reaction gases of the catalytic oxidation of o-xylene and/or naphthalene", *United States Patent*, 1981, **4285871**, 1-22.
- Kirk-Othmer. *Encyclopedia of chemical technology: Acidic and Basic catalysts*, John Wiley & Sons Inc., 1979.
- Larsson, P.O., and Anderson, A., "Oxides of ceria promoted copper, manganese and copper manganese on Al<sub>2</sub>O<sub>3</sub> for the combustion of CO, ethyl acetate and ethanol", *Appl. Catal. B*, 2000, **24**, 175-192.

- Liu, S., Obuchi, A., Uchisawa, J., Nanba, T., and Kushiya, S., "An exploratory study of diesel soot oxidation with NO<sub>2</sub> and O<sub>2</sub> on supported metal oxide catalysts", *Appl. Catal. B*, 2002, **37**, 309-319.
- McCabe, R.W., and Mitchell, P.J., "Oxidation of Ethanol and Acetaldehyde over Alumina-Supported Catalysts", *Ind. Eng. Chem. Prod. Res. Dev.*, 1983, **22**, 212-217.
- McCarty, J.G., Gusman, M., Lowe, D.M., Hildenbran, D.L., and Lau, K.N., "Stability of supported metal and Supported metal oxide combustion catalysts", *Catalysis Today*, 1999, **47**, 5-17.
- Ozkan, U.S., Kueller, R.F., and Moctezuma, E., "Methanol Oxidation over Nonprecious transition Metal Oxide Catalysts", *Ind. Eng. Chem. Res.*, 1990, **29**, 1136-1142.
- Paola, A.D., Lopez, F.G., Ikeda, S., Marci, G., Ohtani, B., and Palmisano, L., "Photocatalytic degradation of organic compounds in aqueous systems by transition metal doped polycrystalline TiO<sub>2</sub>", *Catalysis Today*, 2002, **75**, 87-93.
- Perry, R.H. and Chilton, C.H., *Chemical Engineering Handbook*, 1973.
- Rajesh, H., and Ozkan, U.S., "Complete oxidation of Ethanol, Acetaldehyde, and Ethanol/Methanol Mixtures over Copper Oxide and Copper-chromium Oxide catalysts", *Ind. Eng. Chem. Res.*, 1993, **32**, 1622-1630.
- Reid, R.C., Pranusnitz, J.M., and Poling, B.E., *The Properties of Gases and Liquids*, McGraw-Hill International Book Company, 1988.
- Satterfield, C. N., *Heterogeneous Catalysis in Industrial Practice: Heterogeneous Catalytic Oxidation*, McGraw-Hill, 1980.
- Spivey, J.J., "Complete Oxidation of Volatile Organics", *Ind. Eng. Chem. Res.*, 1987, **26**, 2165-2180.
- Thammanokul, H., "Oxidative dehydrogenation of propane over V-Mg-O catalysts", *Master's Thesis, Faculty of Engineering, Chulalongkorn University*, 1996.
- The JCPDS., *Inorganic Phases Alphabetical Index*, 1980.
- Tongsang, P., "The application of V-Mg-O/TiO<sub>2</sub> catalyst on the combustion of anhydrides", *Master's Thesis, Faculty of Engineering, Chulalongkorn University*, 2001.
- Toyada, Y.; and Teraji, S., "Process for the treatment of byproducts obtained in the preparation of phthalic anhydride" *United States Patent*, 1980, **4181489**, 1-18.

Umpo, S., “The application of Co-Mg-O/Al<sub>2</sub>O<sub>3</sub> catalyst on the combustion of anhydrides”, *Master's Thesis, Faculty of Engineering, Chulalongkorn University*, 2001.

Way, T., and Peter, F., “Apparatus for the recovery of vaporized phthalic anhydride from gas streams” *United States Patent*, 1981, **4252772**, 1-20.

Yao, Y.F.U., “Catalytic oxidation of Ethanol at Low Concentrations” *Ind. Eng. Chem. Process Des. Dev.*, 1984, 23, 60-67.



สถาบันวิทยบริการ  
จุฬาลงกรณ์มหาวิทยาลัย



**APPENDICES**

สถาบันวิทยบริการ  
จุฬาลงกรณ์มหาวิทยาลัย

## APPENDIX A

### CALCULATION OF CATALYST PREPARATION

**Preparation of 8Cr-O/Al<sub>2</sub>O<sub>3</sub>, 8Cr-1Mg-O/Al<sub>2</sub>O<sub>3</sub> and 8Cr-10Mg-O/Al<sub>2</sub>O<sub>3</sub> catalysts by the Wet Impregnation Method is shown as follow:**

Reagent:	- Chromium (III) nitrate nonahydrate [Cr(NO <sub>3</sub> ) <sub>3</sub> ·9H <sub>2</sub> O] Molecular weight = 400.15 g.
	- Magnesium nitrate [Mg(NO <sub>3</sub> ) <sub>2</sub> ] Molecular weight = 256.41 g.
Support	- Alumina [Al <sub>2</sub> O <sub>3</sub> ]

#### **Calculation for the preparation of the 8Cr-O/Al<sub>2</sub>O<sub>3</sub> catalyst.**

The 8Cr-O/Al<sub>2</sub>O<sub>3</sub> aqueous solution used in catalyst preparation consists of Cr 8wt% and Al<sub>2</sub>O<sub>3</sub> 92wt%. The amount of chromium in 8Cr-O/Al<sub>2</sub>O<sub>3</sub> catalyst is calculated as follows:

Basis: Al<sub>2</sub>O<sub>3</sub> 1 g

If the weight of catalyst was 100 g, 8Cr-O/Al<sub>2</sub>O<sub>3</sub> would compose of chromium 8 g and Al<sub>2</sub>O<sub>3</sub> 92 g. Therefore, in this system,

$$\begin{aligned} \text{the amount of Cr} &= 8/92 \times 1 \\ &= 0.08695 \text{ g} \end{aligned}$$

Chromium (Cr) 0.08695 g was prepared from Cr(NO<sub>3</sub>)<sub>3</sub>·9H<sub>2</sub>O 97% and molecular weight of Cr = 51.996, then

$$\begin{aligned} \text{the Cr(NO}_3)_3 \cdot 9\text{H}_2\text{O content} &= (400.15/51.996) \times 0.08695 \times (100/97) \\ &= 0.6898 \text{ g} \end{aligned}$$

### Calculation for the preparation of the 8Cr-1Mg-O/Al<sub>2</sub>O<sub>3</sub> catalyst.

The 8Cr-1Mg-O/Al<sub>2</sub>O<sub>3</sub> aqueous solution used in catalyst preparation consists of Cr 8wt% and Al<sub>2</sub>O<sub>3</sub> 92wt%. The amount of chromium in 8Cr-1Mg-O/Al<sub>2</sub>O<sub>3</sub> catalyst is calculated as follows:

Basis: Al<sub>2</sub>O<sub>3</sub> 1 g

If the weight of catalyst was 100 g, 8Cr-1MgO-/Al<sub>2</sub>O<sub>3</sub> would compose of chromium 8 g and Al<sub>2</sub>O<sub>3</sub> 92 g. Therefore, in this system,

$$\begin{aligned} \text{the amount of Cr} &= 8/92 \times 1 \\ &= 0.08695 \text{ g} \end{aligned}$$

Chromium (Cr) 0.08695 g was prepared from Cr(NO<sub>3</sub>)<sub>3</sub>·9H<sub>2</sub>O 97% and molecular weight of Cr = 51.996, then

$$\begin{aligned} \text{the Cr(NO}_3)_3 \cdot 9\text{H}_2\text{O content} &= (400.15/51.996) \times 0.08695 \times (100/97) \\ &= 0.6898 \text{ g} \end{aligned}$$

Then, the Mg: (support+Cr) weight ratio = 1:100

$$\begin{aligned} \text{The amount of Mg} &= (0.08695+1)/100 \\ &= 0.01087 \text{ g} \end{aligned}$$

Magnesium (Mg) 0.01087 g was impregnated from Mg(NO<sub>3</sub>)<sub>2</sub> solution 99% and molecular weight of Mg = 24.305 g

$$\begin{aligned} \text{The amount of Mg(NO}_3)_2 \text{ used} &= (256.41/24.305) \times 0.01087 \times (100/99) \\ &= 0.1158 \text{ g} \end{aligned}$$

### Calculation for the preparation of the 8Cr-10Mg-O/Al<sub>2</sub>O<sub>3</sub> catalyst.

The 8Cr-10Mg-O/Al<sub>2</sub>O<sub>3</sub> aqueous solution used in catalyst preparation consists of Cr 8wt% and Al<sub>2</sub>O<sub>3</sub> 92wt%. The amount of chromium in 8Cr-10Mg-O/Al<sub>2</sub>O<sub>3</sub> catalyst is calculated as follows:

Basis:  $\text{Al}_2\text{O}_3$  1 g

If the weight of catalyst was 100 g, 8Cr-10Mg-O/ $\text{Al}_2\text{O}_3$  would compose of chromium 8 g and  $\text{Al}_2\text{O}_3$  92 g. Therefore, in this system,

$$\begin{aligned} \text{the amount of Cr} &= 8/92 \times 1 \\ &= 0.08695 \text{ g} \end{aligned}$$

Chromium (Cr) 0.08695 g was prepared from  $\text{Cr}(\text{NO}_3)_3 \cdot 9\text{H}_2\text{O}$  97% and molecular weight of Cr = 51.996, then

$$\begin{aligned} \text{the } \text{Cr}(\text{NO}_3)_3 \cdot 9\text{H}_2\text{O} \text{ content} &= (400.15/51.996) \times 0.08695 \times (100/97) \\ &= 0.6898 \text{ g} \end{aligned}$$

Then, the Mg: (support+Cr) weight ratio = 10:100

$$\begin{aligned} \text{The amount of Mg} &= 10 \times (0.08695 + 1) / 100 \\ &= 0.1087 \text{ g} \end{aligned}$$

Magnesium (Mg) 0.1087 g was impregnated from  $\text{Mg}(\text{NO}_3)_2$  solution 99% and molecular weight of Mg = 24.305 g

$$\begin{aligned} \text{Thus, the amount of } \text{Mg}(\text{NO}_3)_2 \text{ used} &= (256.41/24.305) \times 0.1087 \times (100/99) \\ &= 1.1583 \text{ g} \end{aligned}$$

The calculation for the preparation of other catalysts as follow 8Mn-O/ $\text{Al}_2\text{O}_3$ , 8Mn-1Mg-O/ $\text{Al}_2\text{O}_3$ , 8Mn-10Mg-O/ $\text{Al}_2\text{O}_3$ , 8Mo-O/ $\text{Al}_2\text{O}_3$ , 8Mo-1Mg-O/ $\text{Al}_2\text{O}_3$ , 8Mo-10Mg-O/ $\text{Al}_2\text{O}_3$ , 8W-O/ $\text{Al}_2\text{O}_3$ , 8W-1Mg-O/ $\text{Al}_2\text{O}_3$ , 8W-10Mg-O/ $\text{Al}_2\text{O}_3$ , 8Fe-O/ $\text{Al}_2\text{O}_3$ , 8Fe-1Mg-O/ $\text{Al}_2\text{O}_3$ , 8Fe-10Mg-O/ $\text{Al}_2\text{O}_3$ , 8Zn-O/ $\text{Al}_2\text{O}_3$ , 8Zn-1Mg-O/ $\text{Al}_2\text{O}_3$ , 8Zn-10Mg-O/ $\text{Al}_2\text{O}_3$ , 8Cu-O/ $\text{Al}_2\text{O}_3$ , 8Cu-1Mg-O/ $\text{Al}_2\text{O}_3$ , 8Cu-10Mg-O/ $\text{Al}_2\text{O}_3$ , 8Ni-O/ $\text{Al}_2\text{O}_3$ , 8Ni-1Mg-O/ $\text{Al}_2\text{O}_3$ , 8Ni-10Mg-O/ $\text{Al}_2\text{O}_3$  catalysts were the same as the preparation of 8Cr-O/ $\text{Al}_2\text{O}_3$ , 8Cr-1Mg-O/ $\text{Al}_2\text{O}_3$  and 8Cr-10Mg-O/ $\text{Al}_2\text{O}_3$  catalysts.

## APPENDIX B

### CALCULATION OF DIFFUSIONAL LIMITATION EFFECT

In the present work there are doubt whether the external and internal diffusion limitations interfere with the phthalic anhydride combustion reaction. Hence, the kinetic parameters were calculated based on the experimental data so as to prove the controlled system. The calculation is divided into two parts; one of which is the external diffusion limitation, and the other is the internal diffusion limitation.

#### 1. External diffusion limitation

The phthalic anhydride combustion reaction is considered to be an irreversible first order reaction occurred on the interior pore surface of catalyst particles in a fixed bed reactor. Assume isothermal operation for the reaction.

In the experiment, 0.01% phthalic anhydride, 21% O<sub>2</sub> was used as the unique reactant in the system. Because percentage of phthalic anhydride was rather small compared to the oxygen that it can be neglected. Molecular weight of nitrogen and oxygen are 28.02 and 31.98, respectively. Thus, the average molecular weight of the gas mixture was calculated as follows:

$$\begin{aligned} M_{AB} &= 0.79 \times 28.02 + 0.21 \times 31.98 \\ &= 28.85 \text{ g/mol} \end{aligned}$$

#### Calculation of reactant gas density

Consider the phthalic anhydride combustion is operated at low pressure and high temperature(500°C). We assume that the gases are respect to ideal gas law. The density of such gas mixture reactant at various temperatures is calculated in the following.

$$\rho = PM / RT$$

We obtained :  $\rho = 0.455 \text{ kg/m}^3$

### Calculation of the gas mixture viscosity

The simplified methods for determining the viscosity of low pressure binary are described anywhere (Reid, 1988). The method of Wilke is chosen to estimate the gas mixture viscosity.

For a binary system of 1 and 2,

$$\mu_m = \frac{y_1 \mu_1}{y_1 + y_2 \Phi_{12}} + \frac{y_2 \mu_2}{y_2 + y_1 \Phi_{21}}$$

where  $\mu_m$  = viscosity of the mixture  
 $\mu_1, \mu_2$  = pure component viscosity  
 $y_1, y_2$  = mole fractions

$$\phi_{12} = \frac{\left[ 1 + \left( \frac{\mu_1}{\mu_2} \right)^{1/2} \left( \frac{M_1}{M_2} \right)^{1/4} \right]^2}{\left[ 8 \left( 1 + \frac{M_1}{M_2} \right) \right]^{1/2}}$$

$$\phi_{21} = \phi_{12} \left( \frac{\mu_2}{\mu_1} \right) \left( \frac{M_1}{M_2} \right)$$

$M_1, M_2$  = molecular weight

Let 1 refer to nitrogen and 2 to oxygen

$$M_1 = 28.02 \text{ and } M_2 = 31.98$$

From Perry(1973) the viscosity of nitrogen at 500°C are 0.0368 cP. The viscosity of oxygen at 500°C are 0.039cP.

$$\phi_{12} = 0.971$$

$$\phi_{21} = 0.902$$

$$\mu_m = 3.81 \times 10^{-5} \text{ kg/m-s}$$

### Calculation of diffusion coefficients

Diffusion coefficients for binary gas system at low pressure calculated by empirical correlation are proposed by Reid (1988). Wilke and Lee method is chosen to estimate the value of  $D_{AB}$  due to the general and reliable method. The empirical correlation is

$$D_{AB} = \frac{\left(3.03 - \frac{0.98}{M_{AB}^{1/2}}\right) (10^{-3}) T^{3/2}}{PM_{AB}^{1/2} \sigma_{AB}^2 \Omega_D}$$

where  $D_{AB}$  = binary diffusion coefficient,  $\text{cm}^2/\text{s}$

T = temperature, K

$M_A, M_B$  = molecular weights of A and B, g/mol

$$M_{AB} = 2 \left[ \left( \frac{1}{M_A} \right) + \left( \frac{1}{M_B} \right) \right]^{-1}$$

P = pressure, bar

$\sigma$  = characteristic length,  $\text{\AA}$

$\Omega_D$  = diffusion collision integral, dimensionless

The characteristic Lennard-Jones energy and Length,  $\epsilon$  and  $\sigma$ , of nitrogen and oxygen are as follows: (Reid,1988)

For  $\text{O}_2$  :  $\sigma = 3.467 \text{ \AA}$ ,  $\epsilon/k = 106.7$

For  $N_2$  :  $\sigma = 3.798 \text{ \AA}$  ,  $\varepsilon/k = 71.4$

The sample rules are usually employed.

$$\sigma_{AB} = \frac{\sigma_A + \sigma_B}{2} = \frac{3.798 + 3.467}{2} = 3.63$$

$$\varepsilon_{AB}/k = \left( \frac{\varepsilon_A \varepsilon_B}{k^2} \right)^{1/2} = (71.4 \times 106.7)^{1/2} = 87.28$$

$\Omega_D$  is tabulated as a function of  $kT/\varepsilon$  for the Lennard-Jones potential. The accurate relation is

$$\Omega_D = \frac{A}{(T^*)^B} + \frac{C}{\exp(DT^*)} + \frac{E}{\exp(FT^*)} + \frac{G}{\exp(HT^*)}$$

where  $T^* = \frac{kT}{\varepsilon_{AB}}$  ,  $A = 1.06036$  ,  $B = 0.15610$  ,  $C = 0.19300$  ,  $D = 0.47635$  ,  $E = 1.03587$  ,  $F = 1.52996$  ,  $G = 1.76474$  ,  $H = 3.89411$

Then  $T^* = 8.857$

$$\Omega_D = \frac{1.06036}{(T^*)^{0.15610}} + \frac{0.19300}{\exp(0.47635T^*)} + \frac{1.03587}{\exp(1.52996T^*)} + \frac{1.76474}{\exp(3.89411T^*)}$$

$$\Omega_D = 0.757$$

With Equation of  $D_{AB}$ ,

$$D(N_2-O_2) = 1.123 \text{ m}^2/\text{s}$$

Reactant gas mixture was supplied at 100 ml/min. in tubular microreactor used in the phthalic anhydride oxidation system at 30°C

air flow rate through reactor = 100 ml/min. at 30°C

The density of air ,  $\rho = 1.161 \text{ kg/m}^3$

Mass flow rate =  $1.935 \times 10^{-6}$  kg/s

Diameter of stainless steel tube reactor = 9.5 mm

Cross-sectional area of tube reactor =  $\frac{\pi(9.5 \times 10^{-3})^2}{4} = 7.09 \times 10^{-5}$  m<sup>2</sup>

Mass Velocity , G = 0.027 kg/m<sup>2</sup>-s

Catalyst size = 40-60 mesh = 0.178-0.126 mm

Average catalyst size =  $(0.126+0.178)/2 = 0.152$  mm

Find Reynolds number,  $Re_p$ , which is well known as follows:

$$Re_p = \frac{d_p G}{\mu}$$

We obtained

$$Re_p = 0.108$$

Average transport coefficient between the bulk stream and particles surface could be correlated in terms of dimensionless groups, which characterize the flow conditions. For mass transfer the Sherwood number,  $km\rho/G$ , is an empirical function of the Reynolds number,  $d_p G/\mu$ , and the Schmit number,  $\mu/\rho D$ . The j-factors are defined as the following functions of the Schmidt number and Sherwood numbers:

$$j_D = \frac{k_m \rho}{G} \left( \frac{a_m}{a_t} \right) (\mu / \rho D)^{2/3}$$

The ratio  $(a_m/a_t)$  allows for the possibility that the effective mass-transfer area  $a_m$ , may be less than the total external area,  $a_t$ , of the particles. For Reynolds number greater than 10, the following relationship between  $j_D$  and the Reynolds number well represents available data.

$$j_D = \frac{0.458}{\varepsilon_B} \left( \frac{d_p G}{\mu} \right)^{-0.407}$$

where  $G$  = mass velocity(superficial) based upon cross-sectional area of empty reactor

$$(G = u\rho)$$

$d_p$  = diameter of catalyst particle for spheres

$\mu$  = viscosity of fluid

$\rho$  = density of fluid

$\varepsilon_B$  = void fraction of the interparticle space (void fraction of the bed)

$D$  = molecular diffusivity of component being transferred

Assume  $\varepsilon_B = 0.5$

$$j_D = 2.266$$

A variation of the fixed bed reactor is an assembly of screens or gauze of catalytic solid over which the reacting fluid flows. Data on mass transfer from single screens has been reported by Gay and Maughan. Their correlation is of the form

$$j_D = (\varepsilon k_m \rho / G)(\mu / \rho D)^{2/3}$$

Where  $\varepsilon$  is the porosity of the single screen.

Hence,  $k_m = (j_D G / \rho)(\mu / \rho D)^{-2/3}$

$$k_m = \left( \frac{0.458G}{\varepsilon_B \rho} \right) \text{Re}^{-0.407} \text{Sc}^{-2/3}$$

Find Schmidt number,  $Sc$  :  $Sc = \frac{\mu}{\rho D}$

$$Sc = 7.456 \times 10^{-5}$$

Find  $k_m$  :  $k_m = 75.90 \text{ m/s}$

### Properties of catalyst

Density = 0.375 g/ml catalyst

Diameter of 40-60 mesh catalyst particle = 0.152 mm

$$\text{Weight per catalyst particle} = \frac{\pi(0.152 \times 10^{-1})^3 \times 0.375}{6} = 6.895 \times 10^{-7} \text{ g/particle}$$

External surface area per particle =  $\pi(0.152 \times 10^{-3})^2 = 7.26 \times 10^{-8} \text{ m}^2/\text{particle}$

$$a_m = (7.26 \times 10^{-8}) / (6.895 \times 10^{-7}) = 0.105 \text{ m}^2/\text{gram catalyst}$$

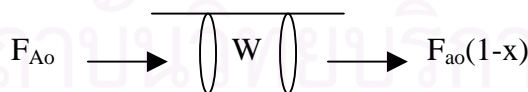
Volumetric flow rate of gaseous feed stream = 100 ml/min

Molar flow rate of gaseous feed stream =  $6.71 \times 10^{-5} \text{ mol/s}$

Phthalic anhydride molar feed rate =  $0.0001 \times 6.71 \times 10^{-5} = 6.71 \times 10^{-9} \text{ mol/s}$

phthalic anhydride conversion (experimental data): 99.80% at 500°C

The estimated rate of phthalic anhydride oxidation reaction is based on the ideal plug flow reactor which there is no mixing in the direction of flow and complete mixing perpendicular to the direction of flow (i.e., in the radial direction). The rate of reaction will vary with reaction length. Plug flow reactors are normally operated at steady state so that properties at any position are constant with respect to time. The mass balance around plug flow reactor becomes



$$\begin{aligned} & \{\text{rate of } i \text{ into volume element}\} - \{\text{rate of } i \text{ out of volume element}\} \\ & + \{\text{rate of production of } i \text{ within the volume element}\} \\ & = \{\text{rate of accumulation of } i \text{ within the volume element}\} \end{aligned}$$

$$\begin{aligned} F_{A_0} &= F_{A_0}(1-x) + (r_W W) \\ (r_W W) &= F_{A_0} - F_{A_0}(1-x) = F_{A_0} x \end{aligned}$$

$$r_w = \frac{F_{AoX}}{W} = 6.70 \times 10^{-10} \text{ mol/s-gram catalyst}$$

At steady state the external transport rate may be written in terms of the diffusion rate from the bulk gas to the surface. The expression is:

$$\begin{aligned} R_{\text{obs}} &= k_m a_m (C_b - C_s) \\ &= \frac{\text{phthalic anhydride converted (mole)}}{(\text{time})(\text{gram of catalyst})} \end{aligned}$$

where  $C_b$  and  $C_s$  are the concentrations in the bulk gas and at the surface, respectively.

$$(C_b - C_s) = \frac{r_{\text{obs}}}{k_m a_m} = 8.407 \times 10^{-11} \text{ mol/m}^3$$

Consider the difference of the bulk and surface concentration is small. It means that the external mass transport has no effect on the phthalic anhydride oxidation reaction rate.

## 2. Internal diffusion limitation

Next, consider the internal diffusion limitation of the phthalic anhydride reaction. An effectiveness factor,  $\eta$ , was defined in order to express the rate of reaction for the whole catalyst pellet,  $r_p$ , in terms of the temperature and concentrations existing at the outer surface as follows:

$$\eta = \frac{\text{actual rate of whole pellet}}{\text{rate evaluated at outer surface conditions}} = \frac{r_p}{r_s}$$

The equation for the local rate (per unit mass of catalyst) may be expected functionally as  $r = f(C, T)$ .

Where  $C$  represents, symbolically, the concentrations of all the involved components

Then,  $r_p = \eta r_s = \eta f(C_s, T_s)$

Suppose that the phthalic anhydride oxidation is an irreversible reaction  $A \rightarrow B$  and first order reaction, so that for isothermal conditions  $r = f(C_A) = k_1 C_A$ . Then  $r_p = \eta k_1 (C_A)_s$ .

For a spherical pellet, a mass balance over the spherical-shell volume of thickness  $\Delta r$ . At steady state the rate of diffusion into the element less the rate of diffusion out will equal the rate of disappearance of reactant within the element. This rate will be  $\rho_p k_1 C_A$  per unit volume, where  $\rho_p$  is the density of the pellet. Hence, the balance may be written, omitting subscript A on C,

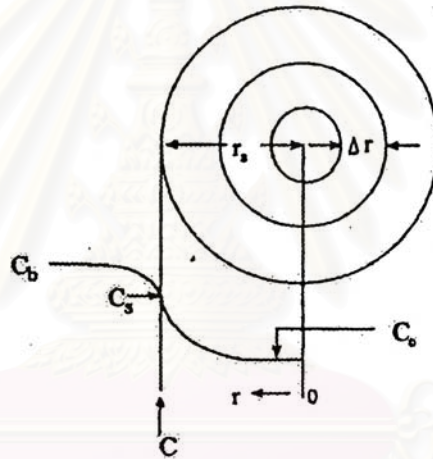


**Figure B1.** Reactant (A) concentration vs. position for first-order reaction on a spherical catalyst pellet.

$$\left( -4\pi r^2 D_e \frac{dC}{dr} \right)_r - \left( -4\pi r^2 D_e \frac{dC}{dr} \right)_{r+\Delta r} = -4\pi r^2 \Delta r_p k_1 C$$

Take the limit as  $\Delta r \rightarrow 0$  and assume that the effective diffusivity is independent of the concentration of reactant, this difference equation becomes

$$\frac{d^2 C}{dr^2} + 2 \frac{dC}{dr} - \frac{k_1 \rho_p C}{D_e} = 0$$

At the center of the pellet symmetry requires

$$\frac{dC}{dr} = 0 \text{ at } r = 0$$

and at outer surface

$$C = C_s \text{ at } r = r_s$$

Solve linear differential equation by conventional methods to yield

$$\frac{C}{C_s} = \frac{r_s \sinh\left(3\phi_s \frac{r}{r_s}\right)}{r \sinh 3\phi_s}$$

where  $\phi_s$  is Thiele modulus for a spherical pellet defined by  $\phi_s = \frac{r_s}{3} \sqrt{\frac{k_1 \rho_p}{D_e}}$

Both  $D_e$  and  $k_1$  are necessary to use  $r_p = \eta k_1 (C_A)_s$ .  $D_e$  could be obtained from the reduced pore volume equation in case of no tortuosity factor.

$$D_e = (\epsilon_s^2 D_{AB})$$

$$D_e = (0.5)^2 (1.123) = 0.281$$

Substitute radius of catalyst pellet,  $r_s = 7.6 \times 10^{-5}$  m with  $\phi_s$  equation

$$\phi_s = 9.253 \times 10^{-7} \sqrt{k} \text{ (dimensionless)}$$

Find  $k$  (at 500°C) from the mass balance equation around plug-flow reactor.

$$r_w = \frac{F_{A0} dx}{dW}$$

where  $r_w = kC_A$

Thus,  $kC_A = \frac{F_{A_0} dx}{dW}$

$$kC_{A_0}(1-x) = \frac{F_{A_0} dx}{dW}$$

$$W = \frac{F_{A_0}}{kC_{A_0}} \int_0^{0.998} \frac{1}{1-x} dx$$

$$k = 0.262 \text{ m}^3/\text{s}\cdot\text{kg catalyst}$$

Calculate  $\phi_s$ :  $\phi_s = 9.253 \times 10^{-7} \sqrt{0.262}$   
 $= 4.74 \times 10^{-7}$

For such small values of  $\phi_s$  it was concluded that the internal mass transport has no effect on the rate of phthalic anhydride oxidation reaction.

สถาบันวิทยบริการ  
 จุฬาลงกรณ์มหาวิทยาลัย

## APPENDIX C

### CALCULATION OF SPECIFIC SURFACE AREA

From Brunauer-Emmett-Teller (BET) equation [Anderson and co-worker (1985)]

$$\frac{p}{n(1-p)} = \frac{1}{n_m C} + \frac{(C-1)p}{n_m C} \quad (C1)$$

Where,  $p$  = Relative partial pressure of adsorbed gas,  $P/P_0$   
 $P_0$  = Saturated vapor pressure of adsorbed gas in the condensed state at the experimental temperature, atm  
 $P$  = Equilibrium vapor pressure of adsorbed gas, atm  
 $n$  = Gas adsorbed at pressure  $P$ , ml. at the NTP/g of sample  
 $n_m$  = Gas adsorbed at monolayer, ml. at the NTP/g of sample  
 $C$  =  $\text{Exp} [(H_C - H_1)/RT]$   
 $H_C$  = Heat of condensation of adsorbed gas on all other layers  
 $H_1$  = Heat of adsorption into the first layer

For the single point method, the graph must pass through the origin. Therefore, the value of  $C$  must be assumed to be infinity.

$C \rightarrow \infty$ , then equation C1 is reduced to

$$\frac{p}{n(1-p)} = \frac{p}{n_m} \quad (C2)$$

The surface area,  $S$ , of the catalyst is given by

$$S = S_b \times n_m \quad (C3)$$

From the gas law

$$\frac{P_b V}{T_b} = \frac{P_t V}{T_t} \quad (C4)$$

Where,  $P_b$  = Pressure at  $0^\circ\text{C}$

$P_t$  = Pressure at  $t^\circ\text{C}$

$T_b$  = Temperature at  $0^\circ\text{C}$  = 273.15 K

$T_t$  = Temperature at  $t^\circ\text{C}$  = 273.15 + t K

V = Constant volume

Then,  $P_b = (273.15/T_t) \times P_t = 1 \text{ atm}$

Partial pressure

$$P = \frac{[\text{Flow of (He + N}_2\text{)} - \text{Flow of He}]}{\text{Flow of (He + N}_2\text{)}} \quad (\text{C5})$$

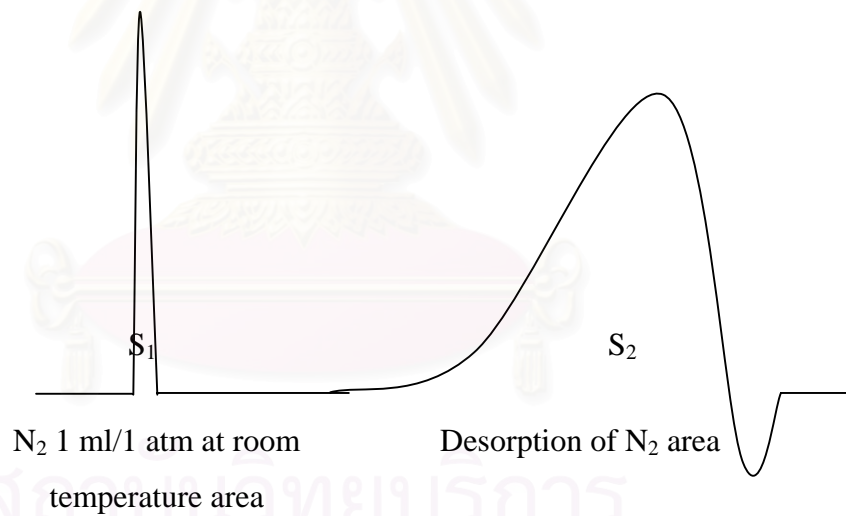
$$= 0.3 \text{ atm}$$

For nitrogen gas, the saturated vapor pressure equals to

$$P_0 = 1.1 \text{ atm}$$

then,  $p = P/P_0 = 0.3/1.1 = 0.2727$

To measure the volume of nitrogen adsorbed, n



$$n = \frac{S_2}{S_1} \times \frac{1}{W} \times \frac{273.15}{T} \text{ ml/g of catalyst} \quad (\text{C6})$$

Where,  $S_1$  =  $\text{N}_2$  1 ml/1 atm at room temperature area

$S_2$  = Desorption of  $\text{N}_2$  area

W = Sample weight, g

T = Room temperature, K

Therefore,

$$n_m = \frac{S_2}{S_1} \times \frac{1}{W} \times \frac{273.15}{T} \times (1-p)$$

$$n_m = \frac{S_2}{S_1} \times \frac{1}{W} \times \frac{273.15}{T} \times 0.7272 \quad (C2.1)$$

Whereas, the surface area of nitrogen gas from literature equal to

$$S_b = 4.373 \text{ m}^2/\text{ml of nitrogen gas}$$

Then,

$$S = \frac{S_2}{S_1} \times \frac{1}{W} \times \frac{273.15}{T} \times 0.7272 \times 4.343$$

$$S = \frac{S_2}{S_1} \times \frac{1}{W} \times \frac{273.15}{T} \times 3.1582 \text{ m}^2/\text{g} \quad (C7)$$

สถาบันวิทยบริการ  
จุฬาลงกรณ์มหาวิทยาลัย

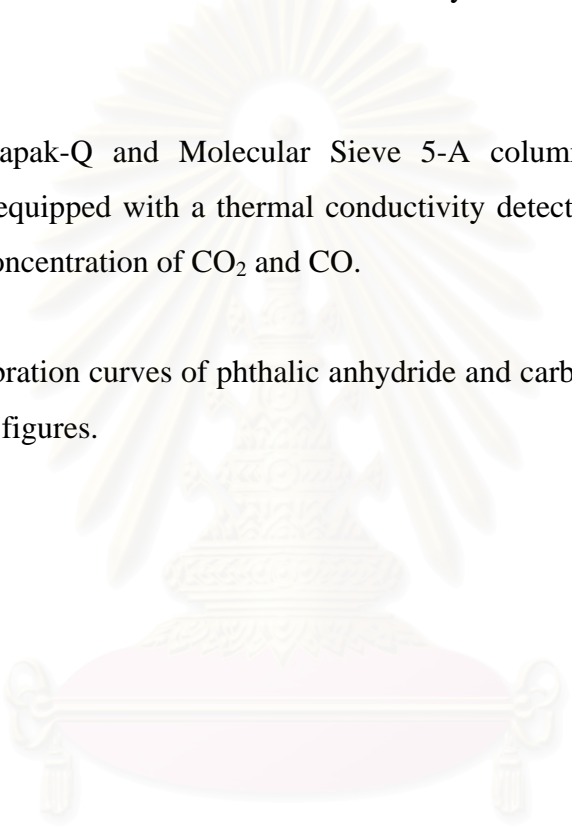
## APPENDIX D

### CALIBRATION CURVE

Flame ionization detector gas chromatographs Shimadzu model 9A equipped with a Chromosorb WAW column is used to analyze the concentrations of phthalic anhydride.

The Porapak-Q and Molecular Sieve 5-A column are used with a gas chromatograph equipped with a thermal conductivity detector, Shimadzu model 8A, to analyze the concentration of CO<sub>2</sub> and CO.

The calibration curves of phthalic anhydride and carbon dioxide are illustrated in the following figures.



สถาบันวิทยบริการ  
จุฬาลงกรณ์มหาวิทยาลัย

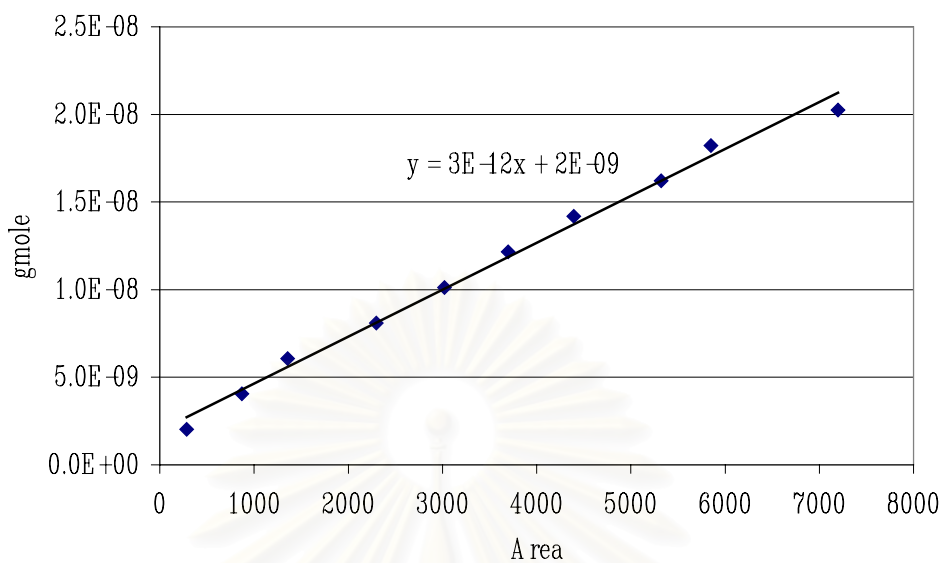


**Figure D1** The calibration curve of phthalic anhydride

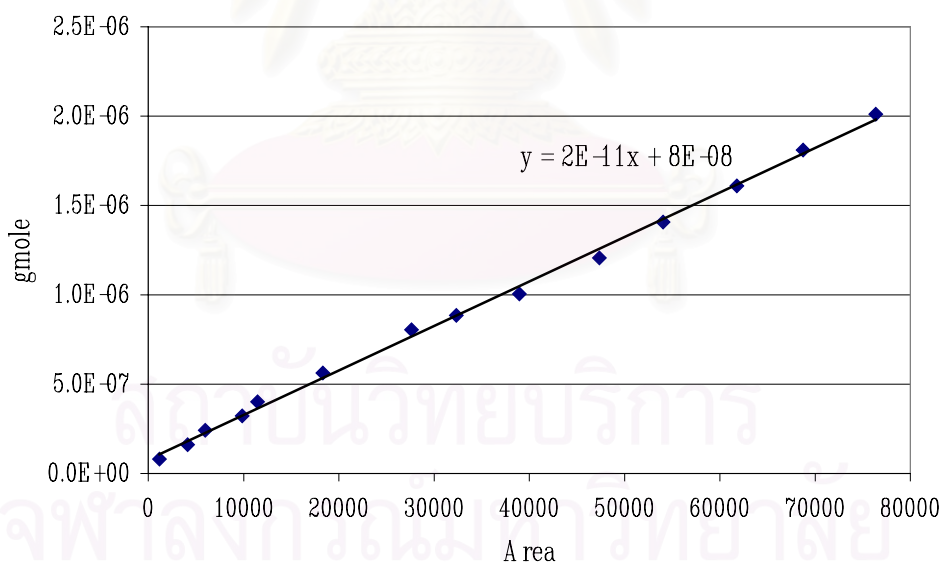


**Figure D2** The calibration curve of carbondioxide

## APPENDIX E

### DATA OF EXPERIMENTS

**Table E1** Data of Figure 5.9

Temp (°C)	Phthalic anhydride conversion (%)		
	8Cr-O/Al <sub>2</sub> O <sub>3</sub>	8Cr-1Mg-O/ Al <sub>2</sub> O <sub>3</sub>	8Cr-10Mg-O/Al <sub>2</sub> O <sub>3</sub>
200	2.85	18.58	2.77
250	16.26	25.63	17.18
280	21.05	31.25	28.22
300	61.31	65.14	50.11
350	77.43	97.88	93.23
400	90.76	98.63	97.15
450	94.36	100	100
500	100	100	100

**Table E2** Data of Figure 5.10

Temp (°C)	Phthalic anhydride conversion (%)		
	8Mn-O/Al <sub>2</sub> O <sub>3</sub>	8Mn-1Mg-O/Al <sub>2</sub> O <sub>3</sub>	8Mn-10Mg-O/Al <sub>2</sub> O <sub>3</sub>
200	0.41	0.84	2.08
250	2.11	2.56	3.92
280	5.43	7.77	8.51
300	14.12	43.66	25.11
350	58.71	95.67	62.56
400	80.10	98.63	100
450	98.87	99.98	100
500	100	100	100

**Table E3** Data of Figure 5.11

Temp (°C)	Phthalic anhydride conversion (%)		
	8Mo-O/Al <sub>2</sub> O <sub>3</sub>	8Mo-1Mg-O/Al <sub>2</sub> O <sub>3</sub>	8Mo-10Mg-O/Al <sub>2</sub> O <sub>3</sub>
200	0.42	0.58	0.98
250	0.53	0.81	1.13
280	2.49	2.53	1.87
300	8.49	33.61	6.21
350	32.45	84.35	43.88
400	72.11	99.02	86.31
450	100	100	99.01
500	100	100	99.12

**Table E4** Data of Figure 5.12

Temp (°C)	Phthalic anhydride conversion (%)		
	8W-O/Al <sub>2</sub> O <sub>3</sub>	8W-1Mg-O/Al <sub>2</sub> O <sub>3</sub>	8W-10Mg-O/Al <sub>2</sub> O <sub>3</sub>
200	5.66	5.57	4.63
250	5.85	8.97	3.92
280	7.66	23.25	8.51
300	16.00	42.79	25.11
350	44.12	84.96	62.56
400	99.19	99.39	100
450	100	99.81	100
500	100	100	100

**Table E5** Data of Figure 5.13

Temp (°C)	Phthalic anhydride conversion (%)		
	8Fe-O/Al <sub>2</sub> O <sub>3</sub>	8Fe-1Mg-O/Al <sub>2</sub> O <sub>3</sub>	8Fe-10Mg-O/Al <sub>2</sub> O <sub>3</sub>
200	1.97	2.73	3.30
250	2.05	2.89	3.85
280	3.51	16.24	4.80
300	8.48	24.16	16.98
350	58.49	78.43	60.91
400	66.14	97.21	89.80
450	97.30	100	99.07
500	99.38	100	99.60

**Table E6** Data of Figure 5.14

Temp (°C)	Phthalic anhydride conversion (%)		
	8Zn-O/Al <sub>2</sub> O <sub>3</sub>	8Zn-1Mg-O/Al <sub>2</sub> O <sub>3</sub>	8Zn-10Mg-O/Al <sub>2</sub> O <sub>3</sub>
200	0.76	1.75	2.99
250	5.55	3.83	5.82
280	11.36	11.19	14.27
300	25.35	38.53	19.11
350	46.50	88.37	71.59
400	87.12	100	100
450	100	100	100
500	100	100	100

**Table E7** Data of Figure 5.15

Temp (°C)	Phthalic anhydride conversion (%)		
	8Cu-O/Al <sub>2</sub> O <sub>3</sub>	8Cu-1Mg-O/Al <sub>2</sub> O <sub>3</sub>	8Cu-10Mg-O/Al <sub>2</sub> O <sub>3</sub>
200	2.01	5.44	3.81
250	40.36	22.65	7.02
280	56.67	50.51	12.70
300	66.27	60.33	33.00
350	87.33	85.23	55.71
400	97.83	92.70	100
450	100	97.81	100
500	100	100	100

**Table E8** Data of Figure 5.16

Temp (°C)	Phthalic anhydride conversion (%)		
	8Ni-O/Al <sub>2</sub> O <sub>3</sub>	8Ni-1Mg-O/Al <sub>2</sub> O <sub>3</sub>	8Ni-10Mg-O/Al <sub>2</sub> O <sub>3</sub>
200	2.78	1.38	0.95
250	10.15	3.52	5.15
280	12.07	5.63	5.42
300	48.20	35.00	17.04
350	96.58	95.06	85.45
400	100	97.86	100
450	100	100	100
500	100	100	100

**Table E9** Data of pyridine and maleic anhydride adsorption of Table 5.3 to 5.5

Metal	Pyridine adsorption			Maleic anhydride adsorption		
	0%Mg	1%Mg	10%Mg	0%Mg	1%Mg	10%Mg
8Cr-O/Al <sub>2</sub> O <sub>3</sub>	112135	97309	58542	1936	2429	3409
8Mn-O/Al <sub>2</sub> O <sub>3</sub>	168684	155828	72265	1413	1956	2891
8Mo-O/Al <sub>2</sub> O <sub>3</sub>	183316	157014	73876	1326	1501	1972
8W-O/Al <sub>2</sub> O <sub>3</sub>	162854	154932	60810	1530	2020	3281
8Fe-O/Al <sub>2</sub> O <sub>3</sub>	55963	51403	41901	2432	3011	4235
8Zn-O/Al <sub>2</sub> O <sub>3</sub>	64356	60498	46499	2085	2650	3834
8Cu-O/Al <sub>2</sub> O <sub>3</sub>	52587	44326	39468	3054	4044	5814
8Ni-O/Al <sub>2</sub> O <sub>3</sub>	51299	41173	37640	4402	4915	6193
Al <sub>2</sub> O <sub>3</sub>	86019			2099		

**APPENDIX F**  
**MATERIAL SAFETY DATA SHEETS OF**  
**PHTHALIC ANHYDRIDE**

**Safety data for phthalic anhydride**

**General**

Synonyms: 1,2-benzenedicarboxylic acid anhydride, phthalic acid anhydride

Molecular formula:  $C_8H_4O_3$

**Physical data**

Appearance: white crystalline solid with choking odour

Melting point: 131°C

Boiling point: 295°C

Vapour density: 5.1 (air=1)

Density ( $g\ cm^{-1}$ ): 1.53

Flash point: 152°C (closed cup)

Explosion limit: 1.7-10.5%

Water solubility: slight

**Stability**

Stable. Combustible. Incompatible with strong oxidizing agents, strong bases, moisture, nitric acid, alkalis. Dust may form an explosive mixture with air.

**Toxicology**

Corrosive - causes burns. Harmful if swallowed or inhaled. Skin or eye contact may cause severe irritation. Typical TLV/TWA 1 ppm. Typical STEL 4 ppm. Typical PEL 2 ppm.

**Personal protection**

Safety glasses, gloves, adequate ventilation.



สถาบันวิทยบริการ  
จุฬาลงกรณ์มหาวิทยาลัย

## APPENDIX G

### PROCEDURE AND CALCULATION OF PYRIDINE AND MALEIC ANHYDRIDE ADSORPTION

#### Pyridine Adsorption

The nitrogen gas flowed through the system that consisted of a tube connected to the gas chromatograph (GC9A). The sample was placed in the tube as shown in Figure G1.

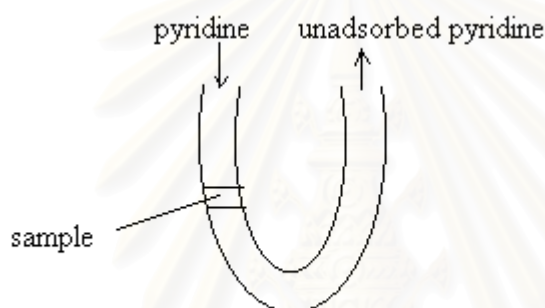


**Figure G1** The adsorption system

The pyridine was injected into the column. The sample would adsorb a part of the pyridine. The pyridine that was not adsorbed on the sample was measured by the gas chromatograph. The pyridine was injected until the peaks were constant. It meant that the sample was saturated with pyridine.

The peaks of the unadsorbed pyridine that were detected from the gas chromatograph were shown in Figure G2.

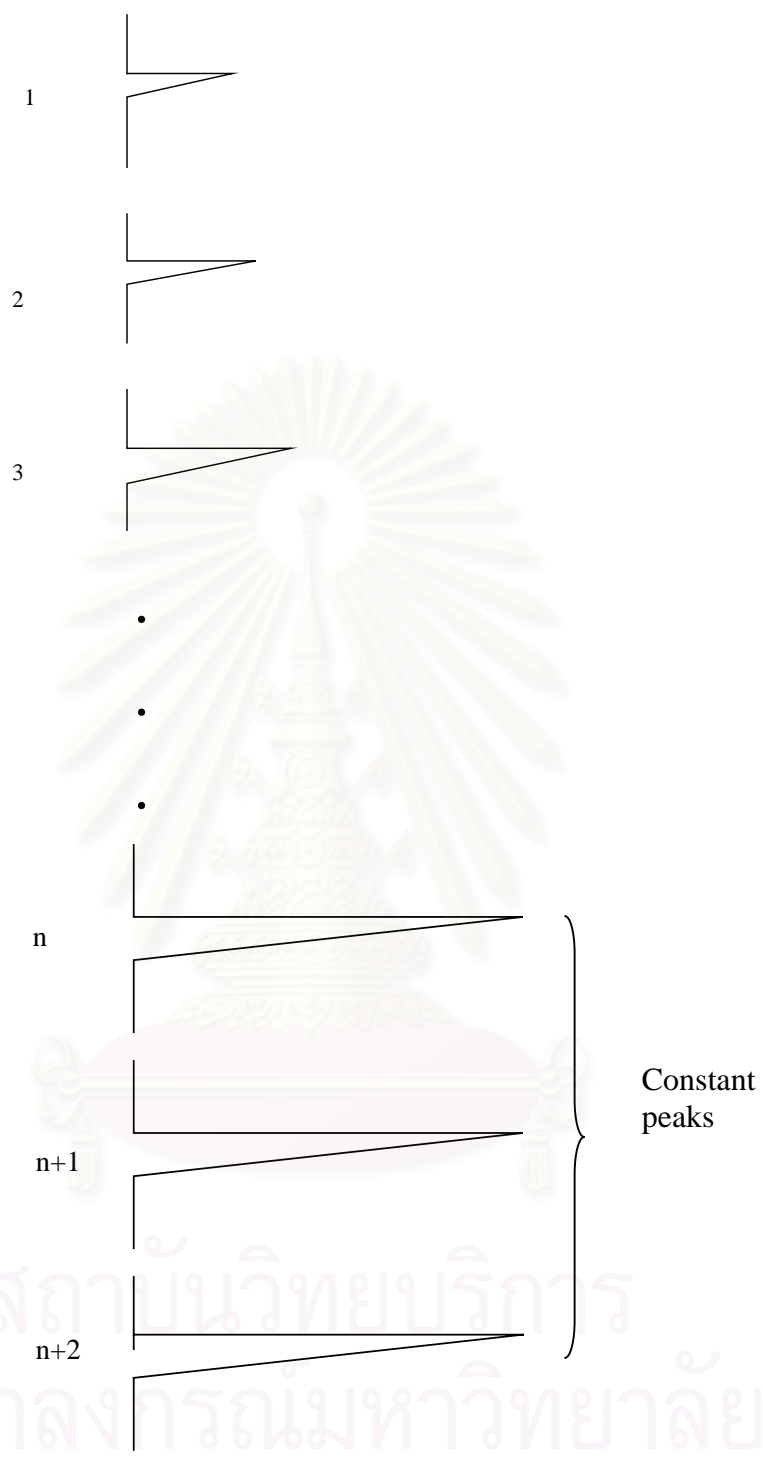


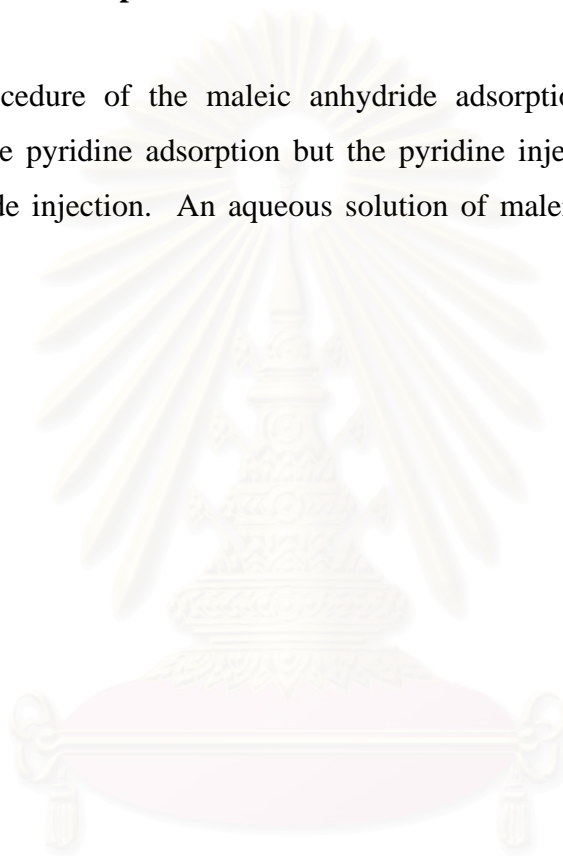
**Figure G2** The unadsorbed pyridine peaks

The overall pyridine adsorbed was calculated by subtraction the area of constant peaks with the 1<sup>st</sup> peak, 2<sup>nd</sup> peak, ..., respectively. The summation of these subtracted areas was the overall area of the pyridine adsorbed.

$$\text{Overall pyridine adsorbed} = \sum (\text{area of constant peak} - \text{area of peak}_i)$$

### **Maleic anhydride adsorption**

The procedure of the maleic anhydride adsorption was the same as the procedure of the pyridine adsorption but the pyridine injection was changed to the maleic anhydride injection. An aqueous solution of maleic anhydride (0.104 g/ml) was used.



สถาบันวิทยบริการ  
จุฬาลงกรณ์มหาวิทยาลัย

## VITA

Miss Jittigan Nugoolchit was born on December 1<sup>st</sup>, 1978 in Nakhonratchasima, Thailand. She received the Bachelor Degree of Chemical Engineering from Faculty of Engineering, Chulalongkorn University in 2001. She continued her Master's Study at Chulalongkorn University in June, 2001.



สถาบันวิทยบริการ  
จุฬาลงกรณ์มหาวิทยาลัย